Cross-Linked Supramolecular Polymer Gels Constructed from Discrete Multi-pillar[5]arene Metallacycles and Their Multiple Stimuli-Responsive Behavior

Zhong-Yu Li,[†] Yanyan Zhang,[‡] Chang-Wei Zhang,[†] Li-Jun Chen,[†] Chao Wang,[§] Hongwei Tan,[∥] Yihua Yu,[‡] Xiaopeng Li,[§] and Hai-Bo Yang*,[†]

[†]Shanghai Key Laboratory of Green Chemistry and Chemical Processes, Department of Chemistry, East China Normal University, Shanghai 200062, P.R. China

[‡]Shanghai Key Laboratory of Magnetic Resonance, Department of Physics, East China Normal University, Shanghai 200062, P.R. China

[§]Department of Chemistry and Biochemistry, Texas State University, San Marcos, Texas 78666, United States

[∥]Department of Chemistry, Beijing Normal University, Beijing 100050, P.R. China

S *Supporting Information*

ABSTRACT: A new family of discrete hexakis-pillar[5]arene metallacycles with different sizes have been successfully prepared *via* coordination-driven self-assembly, which presented very few successful examples of preparation of discrete multiple pillar[n]-arene derivatives. These newly designed hexakis-pillar[5]arene metallacycles were well characterized with one-dimensional (1-D) multinuclear NMR (^{1}H and ^{31}P NMR), two-dimensional (2-D) ^{1}H−^{1}H COSY and NOESY, ESI-TOF-MS, elemental analysis, and PM6 semiempirical molecular orbital methods. Furthermore, the host−guest complexation of such hexakis-pillar[5]arene hosts with a series of different neutral ditopic guests **G1−6** were well investigated. Through host−guest interactions of hexakis-pillar[5]arene metallacycles **H2** or **H3** with the neutral dinitrile guest **G5**, the cross-linked supramolecular polymers **H2⊃(G5)₃** or **H3⊃(G5)₃** were successfully constructed at the high-concentration region, respectively. Interestingly, these cross-linked supramolecular polymers transformed into the stable supramolecular gels upon increasing the concentrations to a relatively high level. More importantly, by taking advantage of the dynamic nature of metal−ligand bonds and host−guest interactions, the reversible multiple stimuli-responsive gel−sol phase transitions of such polymer gels were successfully realized under different stimuli, such as temperature, halide, and competitive guest, etc. The mechanism of such multiple stimuli-responsive processes was well illustrated by *in situ* multinuclear NMR investigation. This research not only provides a highly efficient approach to the preparation of discrete multiple pillar[n]arene derivatives but also presents a new family of multiple stimuli-responsive "smart" soft matters.
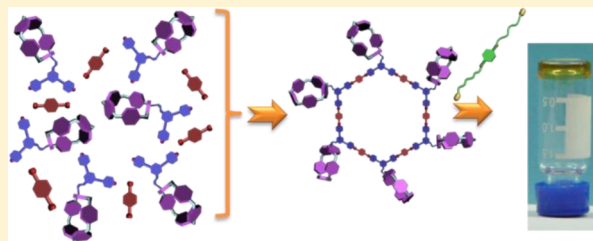
1. INTRODUCTION

One of the most fascinating features of nature is its ability to construct exquisite and complex biological systems from relatively simple molecular precursors through noncovalent interactions.[1] In particular, hierarchical self-assembly, which Sijbesma defined as "a stepwise process in which components are brought together in a precisely defined way by non-covalent interactions",[2c] has been widely explored by nature in the construction of well-organized architectures with the higher level.[2] For instance, the assembly process of the tobacco mosaic virus (TMV) is a typical example that was often enumerated to illustrate the process of hierarchical self-assembly.[3a] Furthermore, collagen fibers are formed through the hierarchical self-assembly of polypeptide chains.[3b] During the past few decades, inspired by such charming natural processes of hierarchical self-assembly, a great number of artificial functional supramolecular systems have been successfully developed and well investigated, thus promoting the investigation of hierarchical self-assembly onto a higher level.[4]

With the development of supramolecular chemistry,[5] coordination-driven self-assembly has gradually evolved to be a controllable and highly efficient methodology for the construction of supramolecular organometallic architectures including two-dimensional (2-D) and three-dimensional (3-D) complexes with well-defined shapes and sizes.[6] The moderate bond energy (15−50 kcal/mol) of metal−ligand bonds, as well as their directional and predictable features, endowed these supramolecular coordination complexes considerable stability yet reversibility.[7] By carefully designing and selecting precursors with appropriate angles, a great number of discrete supramolecular organometallic polygons have been successfully

obtained such as squares, rhomboids, triangles, hexagons, etc., some of which have exhibited wide applications in the area of catalysis, sensors, supramolecular devices, etc.[8] Owing to the well-defined core structures of such metallacycles, multiple functional moieties can be easily introduced onto the predesigned metallacyclic skeletons, thus providing the possible secondary interactions for hierarchical self-assembly. For example, the highly ordered supramolecular nanostructures were successfully obtained via hierarchical self-assembly of discrete rhomboidal metallacycles.[9] However, the hierarchical self-assembly based on metal–ligand coordination bonds and host–guest interactions has been rarely investigated. Particularly, to the best of our knowledge, there are very few examples of the cross-linked supramolecular polymers with multiple stimuli-responsive features prepared through the hierarchical self-assembly involving both metal–ligand coordination and host–guest interactions.

It is well-known that macrocyclic chemistry established the foundation of modern supramolecular chemistry. Moreover, the molecular recognition based on macrocyclic host molecules has always been one of the most attractive fields within supramolecular chemistry.[10] As a new family of macrocyclic host molecules, which was first reported by Ogoshi in 2008,[11a] pillar[n]arenes have gradually developed into the new driving force to stimulate the development of supramolecular chemistry.[11] It should be noted that pillar[n]arenes feature a relatively more rigid and symmetrical cavity structure compared to the traditional calix[n]arenes due to the difference in the connection of their repeating units. Furthermore, pillar[n]-arenes are relatively easy to be functionalized through the reasonable design and control of synthetic method.[12] These intrinsic characteristics determine the pillar[n]arenes as excellent host molecules, which can not only complex with different cationic molecules,[13a–e] but also recognize neutral guests.[13f–h] In addition to the construction of mechanically interlocked structures through host–guest interactions,[12e,14] pillar[n]arenes have also been extensively explored in the areas of functional supramolecular systems.[15–17] For example, a new family of MOF materials was successfully prepared from difunctionalized pillar[5]arene derivatives by Stoddart's group.[18] A variety of supramolecular polymers based on pillar[n]arene analogues were constructed through the reasonable design of the host and guest structures.[12d,19]

Recently, considerable research interest has been devoted to the design and synthesis of multiple pillar[n]arene derivatives, which present promising applications in multicomponent host–guest recognition and the construction of the higher-order complexes.[19c,d,20] However, there have been very few successful examples on the preparation of discrete multiple pillar[n]arene analogues in literature, which might be caused by the obstacle of the conventional covalent synthetic strategies. Up to now, Zhao and co-workers have reported the only example of tris-pillar[5]arene derivative.[20d] Thus, it is extremely necessary to explore an efficient strategy for the preparation of discrete multi-pillar[n]arene species.

By taking advantage of the controllability and high efficiency of coordination-driven self-assembly,[21] a large number of well-defined metallacycles decorated with different multiple functional moieties (e.g., crown ether, ferrocene, diarylethene, pyrene, and Fréchet-type dendrons, etc.) have been successfully prepared.[22] Stimulated by these successful examples, we envisioned that the construction of the discrete multiple pillar[n]arene derivatives with well-designed shapes and sizes

would be realized by selecting suitable monofunctionalized pillar[n]arene species and the corresponding building blocks with proper angle and symmetry. In addition, the possibility to fine-tune the size and shape of the final metallacycles substituted with multiple pillar[n]arene moieties would provide the enhanced understanding of the geometrical requirements necessary for molecular self-assembly. Furthermore, this strategy would likely give rise to the design and synthesis of novel supramolecular materials with inspired functionality arising from their unique interior rings and multiple pillar[n]-arene exteriors.

Herein, we report the construction of a new family of hexakis-pillar[5]arene metallacycles via coordination-driven self-assembly. A new 120° pillar[5]arene containing dipyridyl donor was designed and successfully prepared. When the newly designed 120° pillar[5]arene derivatives were combined with the corresponding complementary 180° di-Pt(II) acceptors with different lengths, two different sized hexakis-pillar[5]arene metallacycles were obtained via coordination-driven self-assembly in one step and in nearly quantitative yield. Subsequently, the investigation of the host–guest chemistry of hexakis-pillar[5]arene metallacycles with different neutral ditopic guests was carried out. It was found that the cross-linked supramolecular polymers were constructed from hexakis-pillar[5]arene metallacycles mainly based on host–guest interactions. Notably, the cross-linked supramolecular polymers could further form supramolecular polymer gels at higher concentrations. More importantly, because of the dynamic nature of hierarchical self-assembly, the reversible gel–sol transitions were successfully realized through the disassembly and reassembly of such cross-linked supramolecular polymer networks stimulated by various external stimuli including temperature, halide, and competitive guest, etc. It should be noted that, although the controlled self-assembly and disassembly has been extensively explored in the area of supramolecular polymers,[23,24] there have been very few reports on multiple stimuli-responsive supramolecular polymer gels derived from multi-pillar[n]arene derivatives through hierarchical self-assembly up to now.

2. RESULTS AND DISCUSSION

Self-Assembly of the Hexakis-Pillar[5]arene Metallacycles H2 and H3. In general, according to the design principles of coordination-driven self-assembly,[6f] the size and shape of the final discrete metallacycles are usually determined by the angle of the selected building blocks. For example, the combination of six 120° building blocks and six linear linkers (180° building blocks) can result in the formation of a discrete hexagonal metallacycle.[8e,f,25] In this study, a new 120° monofunctionalized pillar[5]arene dipyridyl donor H1 and 180° linear di-Pt(II) acceptors with different lengths were selected for the construction of hexakis-pillar[5]arene metallacycles H2 and H3, respectively.

The 120° pillar[5]arene containing dipyridyl donor H1 was easily synthesized through an esterification reaction of the pillar[5]arene acid 1[19e] and 3,5-bis(4-ethynlpyridinyl)phenol 2[8d] in the presence of EDCI and HOBt as presented in Scheme 1. With the aim to construct the multiple pillar[5]arene metallacycles with different sizes, two linear di-Pt(II) acceptors 3 and 4 with different lengths were employed,[25c] respectively. Stirring the mixtures of the 120° monopillar[5]arene donor ligand H1 with the differently sized linear di-Pt(II) acceptors 3 or 4 in the stoichiometric ratio in a mixed solvent of CH_2Cl_2

Scheme 1. Synthesis of 120° Monofunctionalized Pillar[5]arene Dipyridyl Donor H1
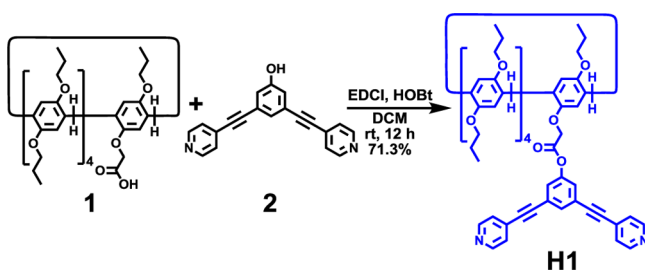
and acetone led to the formation of self-assemblies **H2** or **H3**, respectively (Scheme 2 and Supporting Information (SI) Schemes S2 and S3). Then the multiple pillar[5]arene derivatives **H2** and **H3** were dissolved in dichloromethane-d_2 for ^{1}H and ^{31}P NMR studies.

Multinuclear NMR (^{1}H and ^{31}P) analysis of the assemblies **H2** and **H3** revealed the formation of discrete multi-pillar[5]arene metallacycles with highly symmetric structures. For instance, both ^{31}P{^{1}H} NMR spectra of **H2** and **H3** displayed a sharp singlet (~13.17 ppm for **H2** and 13.92 ppm for **H3**), which shifted upfield from the starting 180° di-Pt(II) acceptors **3** or **4** by approximately 6.20 ppm. This change, as well as the decrease in coupling of flanking ^{195}Pt satellites (~$\Delta J \approx -160.3$ Hz for **H2** and $\Delta J \approx -153.8$ Hz for **H3**), is consistent with the electron back-donation from the platinum atoms (Figure 1A). Moreover, as shown in Figure 1B, the ^{1}H NMR spectrum of the small multi-pillar[5]arene metallacycle **H2** displayed the downfield shifts of the pyridyl proton signals compared with the 120° mono-pillar[5]arene dipyridyl donor **H1** (for α-H, $\Delta\delta \approx 0.08$ ppm; for β-H, $\Delta\delta \approx 0.42$ ppm), associated with the loss of electron density upon coordination by the nitrogen lone pair to platinum metal centers. Similarly, in the ^{1}H NMR spectrum of the large multi-pillar[5]arene metallacycle **H3**, the α- and β-pyridyl hydrogen signals both exhibited the obvious downfield shifts (for α-H, $\Delta\delta \approx 0.09$

ppm; for β-H, $\Delta\delta \approx 0.43$ ppm), which were attributed to the formation of nitrogen–platinum (N–Pt) bonds as well.

Further characterization by 2-D ^{1}H NMR spectroscopic techniques (^{1}H–^{1}H COSY and NOESY) are in agreement with the formation of the discrete multi-pillar[5]arene metallacycles (Figures S63–S64 in SI). For instance, the presence of cross-peaks between the signals of the pyridine protons (α-H and β-H) and the PEt$_3$ protons (CH$_2$ and CH$_3$) were found in the 2-D NOESY spectrum, which supported the construction of multi-pillar[5]arene metallacycles based on the formation of N–Pt bonds (Figures S63b and S64b in SI). The sharp NMR signals in both ^{31}P and ^{1}H NMR spectra along with the solubility of these species ruled out the formation of oligomers.

Mass spectrometric studies of multi-pillar[5]arene metalla-cycles **H2** and **H3** were performed by using electrospray ionization time-of-flight mass spectrometry (ESI-TOF-MS), which allows the assemblies to remain intact during the ionization process while obtaining the high resolution required for isotopic distribution. The ESI-MS-TOF analysis provided the further strong support for the existence of multi-pillar[5]arene metallacycles. In fact, it is very challenging to determine the accurate mass for these charged metallacycles as a result of the large molecular weight and isotopic shift. The ESI-TOF-MS spectrum of **H2** revealed two peaks at m/z = 1248.7319 and 2047.3915, corresponding to $[\mathbf{M} - 11\mathrm{OTf}]^{11+}$ and $[\mathbf{M} - 7\mathrm{OTf}]^{7+}$ species, where M represents the intact assemblies, respectively. These peaks were isotopically resolved (Figure 2A) and agreed very well with their theoretical distribution. Compared to the small hexakis-pillar[5]arene metallacycle **H2**, it is more difficult to get strong mass signals for the large metallacycle **H3** even under the ESI-TOF-MS conditions on account of its larger molecular weight (15821.7424 Da). With considerable effort, the peaks at m/z = 1290.2201 and 2112.6904 attributable to $[\mathbf{M} - 11\mathrm{OTf}]^{11+}$ and $[\mathbf{M} - 7\mathrm{OTf}]^{7+}$ species, respectively, were found in the ESI-TOF-MS spectrum of **H3** (Figure 2B). All of the these peaks were isotopically resolved, and they are in good agreement with their theoretical distributions, which allowed for the molec-

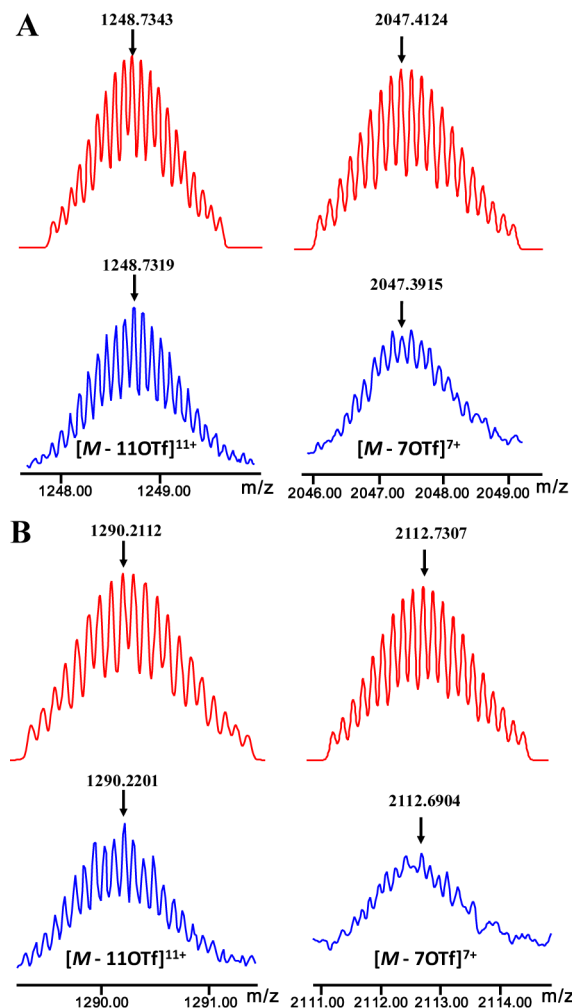**Scheme 2. Graphical Representation of the Self-Assembled Hexakis-Pillar[5]arene Metallacycles H2 and H3**
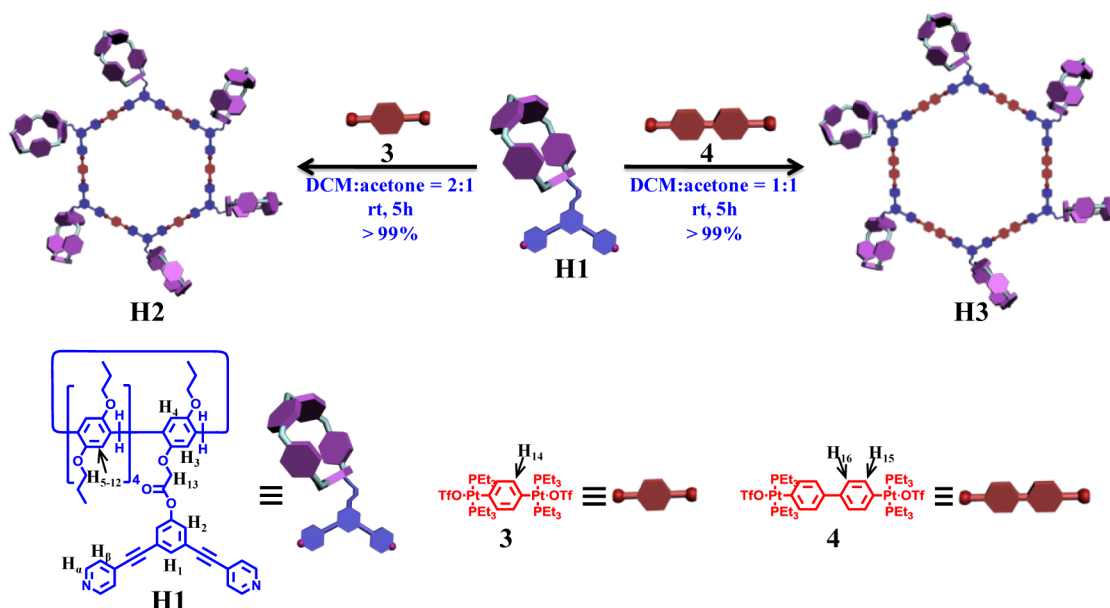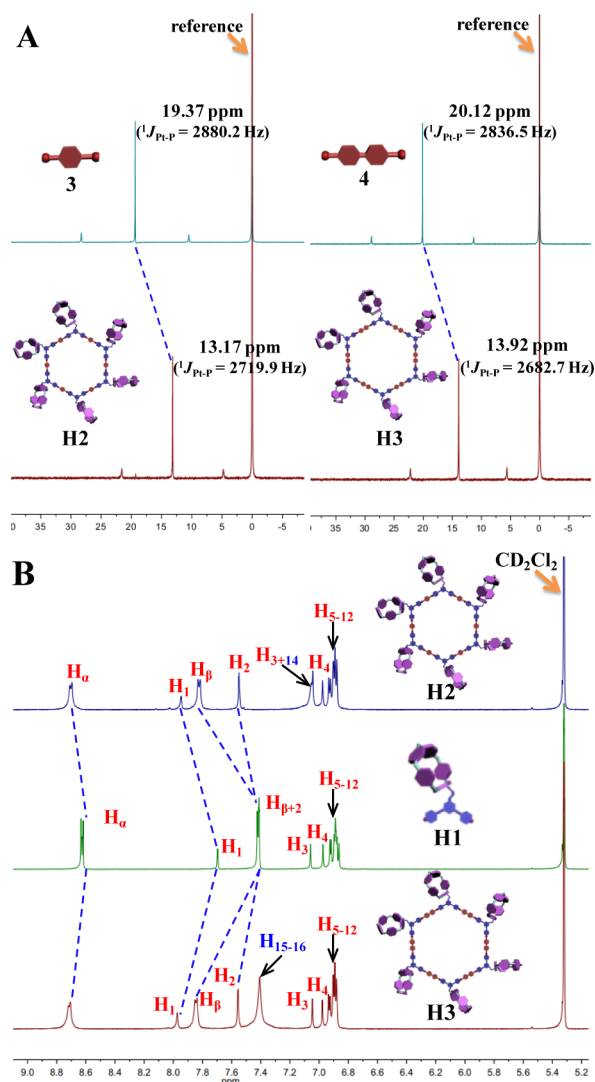
Figure 1. (A) ^{31}P NMR spectra (400 MHz, 295 K) of 180° acceptors **3,4** and metallacycles **H2**, **H3** in CD_2Cl_2. (B) Partial ^{1}H NMR spectra (400 MHz, 295 K) of small metallacycle **H2**, 120° donor ligand **H1**, and large metallacycle **H3** in CD_2Cl_2.

Figure 2. Theoretical (top) and experimental (bottom) ESI-TOF-MS spectra of multi-pillar[5]arene metallacycles **H2** (A) and **H3** (B).

Figure 3. The geometry structures of the hexakis-pillar[5]arene metallacycles **H2** (A) and **H3** (B) optimized by PM6 semiempirical molecular orbital method.
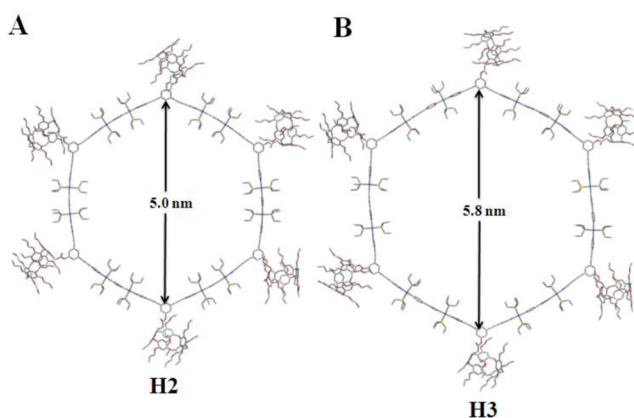
ularity of the hexakis-pillar[5]arene metallacycles to be unambiguously established.

All attempts to grow X-ray-quality single crystals of these hexakis-pillar[5]arene metallacycles have so far proven unsuccessful. Therefore, the PM6 semiempirical molecular orbital method was employed to gain further insight into the structural characteristics of these multi-pillar[5]arene derivatives (Figure 3 and SI Figures S1−S2). Molecular simulation indicated that both hexakis-pillar[5]arene metallacycles **H2** and **H3** featured a very similar, roughly planar hexagonal ring at their core surrounded by six rigid pillar[5]arenes. Moreover, the simulations revealed the internal diameters of 5.0 and 5.8 nm for **H2** and **H3**, respectively.

Host−Guest Complexation Studies of Hexakis-pillar[5]arene with Neutral Ditopic Guests in Dilute Solution. During the past few years pillar[n]arenes have been recognized as exceptionally versatile hosts for a wide variety of guests. Although the initial studies focused primarily upon the cationic species,[13a−e] more recently, the host−guest complex-ation studies of pillar[n]arene derivatives with neutral guests in organic media have received considerable attention.[13f−h] Some

successful experimental investigations have demonstrated that the appropriately sized pillar[5]arene derivatives bound some neutral guests both in solution and the solid state in a threaded manner. Moreover, the high affinity binding and molecular recognition motifs operative in the complexation between different pillar[5]arenes and neutral guests are well established and understood. For example, Li and co-workers reported that

the combination of complementary pillar[5]arene host and dinitrile guest in a 1:1 molar ratio resulted in the formation of a pseudorotaxane complex mainly driven by dipole−dipole forces.[13g] Additional [C−H···π] and [C−H···N] and [C−H···O] hydrogen bonding further contributed to the stability of the resultant host−guest complexes. By taking advantage of the strong affinities of pillar[5]arenes with neutral guests in organic solvents, we envisioned that a new class of cross-linked supramolecular polymers could be prepared from the newly designed hexakis-pillar[5]arene metallacycles *via* host−guest interactions when the neutral ditopic molecules were employed as guests. More importantly, owing to the dynamic and reversible nature of noncovalent interactions, such supramolecular polymers might be endowed with new functions such as reversibility and stimuli-responsiveness.

With these novel hexakis-pillar[5]arene metallacycles in hand, an investigation of the host−guest complexation with the neutral ditopic guests in dilute solution was first carried out. A series of neutral ditopic guests **G1−6** (Figure 4) have been
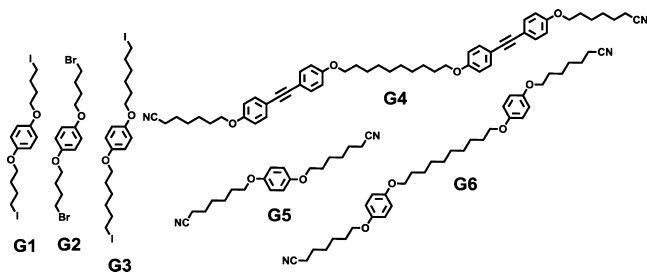

Figure 4. Molecular structures of different neutral ditopic halide guests **G1−3** and dinitrile guests **G4−6**.

designed and successfully synthesized (Schemes S4−S6 in SI). Neutral halide ditopic guests **G1−3** have different length and halogen atoms, while the neutral ditopic nitrile guests **G4−6** feature different sizes and solubility. The complexation of monofunctionalized pillar[5]arene **H1** with the ditopic guests **G1−6** was first studied by ^{1}H NMR spectroscopy, respectively. The dinitrile guest **G5** was selected as a representative. As shown in Figure S12 in SI, when 2.0 equiv of host **H1** was added into an acetone-d_6 solution of **G5** (3.0 mM), the signals related to the protons on guest **G5** exhibited obvious broadening effects compared to the free axle. For example, the resonance peak related to protons H_c of **G5** disappeared after the complexation caused by the broadening effect, and a new broad peak was found in the upfield region, indicating that the pillar[5]arene cavity was threaded by the guest molecule.[13g,h,19d] In addition, it was found that the phenyl protons H_3 and H_4 on **H1** shifted downfield from 7.174 to 7.210 ppm and 6.975 to 7.012 ppm, respectively, accompanied by a slight broadening effect. Moreover, the methylene proton H_{13} on **H1** was found to shift downfield from 4.952 to 4.964 ppm. All obtained results supported that the linear long chain part of ditopic guest **G5** was threaded through the cavity of host **H1** to form host−guest complexation in solution, which has been well illustrated by Li's group.[13g,19c,d] Similarly, the ditopic guest **G6** was proved to be complexed by **H1** as well (Figure S15 in SI). Moreover, the neutral ditopic halide guests **G1−3** exhibited fast-exchange complexation with the monofunctionalized pillar[5]arene **H1** in the ^{1}H NMR time scale at 295 K in acetone-d_6 (Figures S3, S6, and S9 in SI), which is similar to the previous report by Li's group. Interestingly,

although dinitrile guest **G5** features the best solubility among **G1−6**, the complex **H1⊃G5** was dissolved out and formed a white precipitate after mixing the monofunctionalized pillar[5]-arene **H1** with dinitrile guest **G5** in acetone even at relatively low concentration (pillar[5]arene unit, 6.5 mM).

It should be noted that the neutral ditopic guest **G4** has a very poor solubility in acetone, so the investigation of the host−guest complexation between monofunctionalized pillar[5]arene **H1** and **G4** was performed in dichloromethane. However, as indicated in ^{1}H NMR spectra in CD₂Cl₂ in Figure S18 in SI, the host **H1** had relative weak complexation ability with the guest **G4**. A possible reason is that the pillar[5]arene preferred to bind to the dichloromethane molecule rather than guest **G4** because the size of pillar[5]arene cavity is more suitable for the dichloromethane molecule.[26] Similarly, it was found that monofunctionalized pillar[5]arene **H1** was not able to complex with other ditopic guests **G1−3**, **G5**, and **G6** or had weak complexation in dichloromethane (Figures S19−S23 in SI). Moreover, as shown in Figure S23 in SI, in the ^{1}H NMR spectra of the complex **H1⊃G3** in acetone-d_6, upon adding CD₂Cl₂, the proton signals of free **G3** gradually became obvious, indicating that the host−guest interaction between monofunctionalized pillar[5]arene **H1** and neutral ditopic guest **G3** in acetone-d_6 was gradually weakened with the addition of CD₂Cl₂. This result again demonstrated that the dichloromethane molecules can occupy the cavity of pillar[5]arene and prevent the complexation between pillar[5]arene with neutral guests.

Subsequently, the host−guest complexation studies of hexakis-pillar[5]arene metallacycles **H2** and **H3** with different ditopic guests **G1−6** in acetone were carried out. Similarly, the guest **G5** was selected as a representative to illustrate the host−guest complexation of hexakis-pillar[5]arene metallacycles with neutral ditopic guests. Since the different mole ratio between multi-pillar[5]arene hosts and ditopic guests may generate different poly[2]pseudorotaxanes combinatorial library, the 1:1 mol ratio between pillar[5]arene unit with the guest binding site (that is, **H2:G5** = 1:3; **H3:G5** = 1:3) was employed in this study, which may prefer to the formation of tris[2]-pseudorotaxanes at the low concentration. As indicated in ^{1}H NMR spectra, with the addition of 3.0 equiv of guest **G5** into an acetone-d_6 solution of **H2** or **H3**, phenyl protons H_3 and H_4 on **H2** shifted downfield from 7.150 to 7.192 ppm and 6.987 to 7.013 ppm, while phenyl protons H_3 and H_4 on **H3** shifted downfield from 7.151 to 7.207 ppm and 6.990 to 7.027 ppm, respectively, both accompanied with a slight broadening effect (Figure 5 and Figures S13−S14 in SI). Moreover, the methylene protons H_{13} on **H2** and **H3** also shifted slightly downfield from 4.964 to 4.978 ppm and 4.970 to 4.992 ppm, respectively. In addition, the resonance peak related to protons H_c of guest **G5** disappeared after the complexation caused by a broadening effect, and a new broad peak was found in the upfield location. All obtained results indicated that the linear long chain of ditopic guest **G5** was threaded through the cavity of pillar[5]arene on host **H2** or **H3** to form host−guest complexes in solution. In this study, **H2⊃(G5)₃** and **H3⊃(G5)₃** were used to represent these host−guest systems because the molar ratio between macrocyclic host **H2** or **H3** and neutral ditopic guest **G5** was 1:3, respectively. It should be noted that, compared to the poor solubility of the complex of **H1⊃G5**, the solubility of complex **H2⊃(G5)₃** or **H3⊃(G5)₃** was improved significantly. It was found that the complex **H2⊃(G5)₃** or **H3⊃(G5)₃** formed a clear, yellow solution even
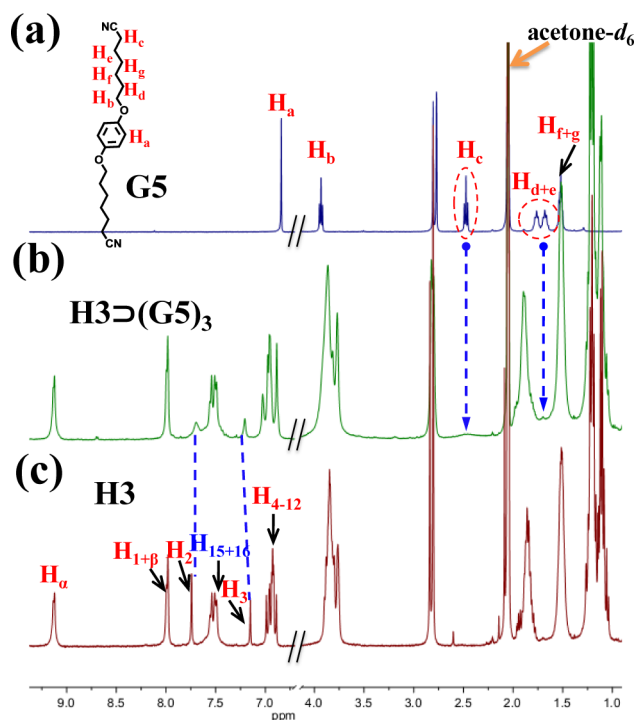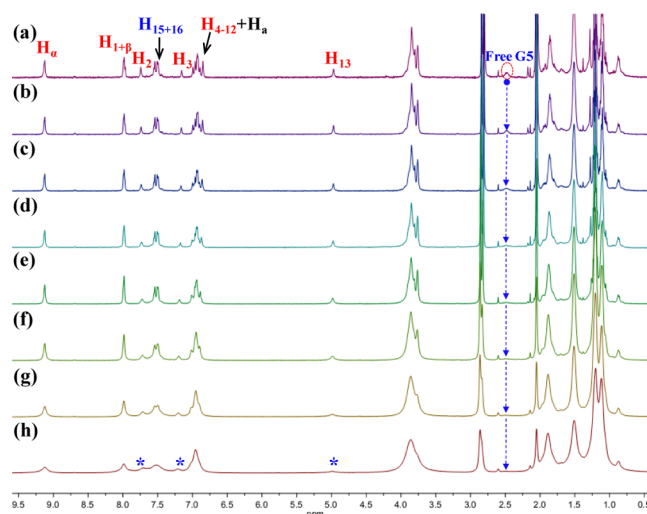
Figure 5. ^{1}H NMR spectra (400 MHz, acetone-d_6, 295 K) of (a) 3.0 mM **G5**, (b) 3.0 mM **G5** + 1.0 mM **H3**, and (c) 1.0 mM **H3**.

Figure 6. ^{1}H NMR spectra of **H3⊃(G5)$_3$** (500 MHz, acetone-d_6, 295 K) at different concentrations: (a) 0.6 mM, (b) 1.0 mM, (c) 2.0 mM, (d) 4.0 mM, (e) 8.0 mM, (f) 12.0 mM, (g) 16.4 mM, (h) 20.0 mM.

at relatively high concentration. Similarly, different poly[2]-pseudorotaxanes based on other neutral ditopic guests **G1−3** and **G6** were well investigated through ^{1}H NMR spectroscopy as well (Figures S4−S5, S7−S8, S10−S11, and S16−S17 in SI).

Cross-Linked Supramolecular Polymers Constructed through Host–Guest Interactions. Encouraged by the recognition motif between the hexakis-pillar[5]arene metalla-cycles hosts **H2** or **H3** and the neutral ditopic guest **G5** along with their good solubility in acetone, the mixtures of **H2** or **H3** with the ditopic guest **G5** (1:3 molar ratio of **H2** and **G5** or **H3** and **G5**) at high concentration was expected to form a new family of cross-linked supramolecular polymers **H2⊃(G5)$_3$** or **H3⊃(G5)$_3$**, respectively. The concentration-dependent ^{1}H NMR spectra of complexes **H2⊃(G5)$_3$** and **H3⊃(G5)$_3$** demonstrated the formation of such cross-linked supra-molecular polymers. For instance, ^{1}H NMR spectra (500 MHz, acetone-d_6, 295 K) of the complex of **H3** and **G5** in a 1:3 molar ratio over a range of pillar[5]arene unit concentrations from 0.6 up to 20 mM were recorded with the purpose of probing the process of the supramolecular polymer formation (Figure 6). At low concentration (<2.0 mM), no obvious signal broadening was found, indicating that poly[2]pseudorotaxanes predominated in solution at low concentration. Upon increasing the concentration, the signal of free **G5** gradually became unobvious and finally disappeared. Moreover, the ^{1}H NMR spectra revealed a slight downfield shift of H_{13} on pillar[5]arene of **H3**. Particularly, it was found that all main peaks of **H3⊃(G5)$_3$** broadened markedly. Likewise, the similar concentration-dependent ^{1}H NMR experimental results were found for **H2⊃(G5)$_3$**, which supported the formation of analogous cross-linked supramolecular polymers through host–guest interactions as well (Figure S24 in SI).

Moreover, 2-D diffusion-ordered NMR spectroscopy (DOSY) experiments were performed to provide further evidence for the formation of cross-linked supramolecular

polymers. For instance, it was found that the increase of the concentration of **H2⊃(G5)$_3$** from 2.0 to 20.0 mM resulted in the decrease of the measured weight-average diffusion coefficients D from 1.88×10^{-10} to 2.80×10^{-12} m^2 s^{-1} ($D_{2.0\ mM}/D_{20.0\ mM} = 67.1$), as shown in the plot of diffusion coefficient against concentration (Figure 7A). Similarly, as the
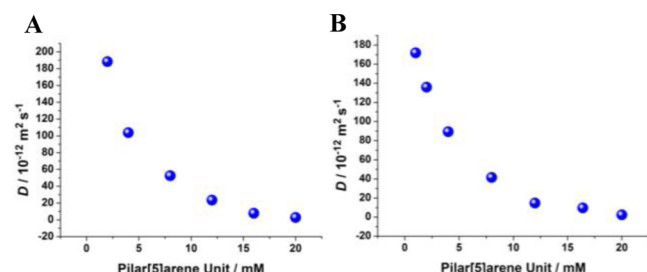

Figure 7. 2-D DOSY (500 MHz, 295 K) plot of solutions in acetone-d_6 of 1:3 molar ratio of **H2** and **G5** (A) and 1:3 molar ratio of **H3** and **G5** (B) at different concentrations, respectively.

concentration of **H3⊃(G5)$_3$** increased from 1.0 to 20.0 mM, the D value decreased from 1.72×10^{-10} to 2.36×10^{-12} m^2 s^{-1} ($D_{1.0\ mM}/D_{20.0\ mM} = 72.9$) (Figure 7B). In general, a more than 10-fold decrease of the diffusion coefficient is believed to be important evidence for the formation of a polymerization with high degree.[24e] Thus, the obtained results strongly support the formation of extended, cross-linked supramolecular polymers. Moreover, the current DOSY experimental results further revealed that the generation of such supramolecular polymers was somewhat concentration dependent.

With the aim of obtaining the further evidence for the existence of cross-linked supramolecular polymers, dynamic light-scattering (DLS) measurements were carried out to investigate the size distributions of the generated supra-molecular aggregates of **H2⊃(G5)$_3$** and **H3⊃(G5)$_3$** at 6.00 mM in acetone, respectively (Figure S25 in SI). It was found that the large-sized cross-linked supramolecular polymers were formed with the hydrodynamic diameter (D_h) value from 220 − 615 nm. Meanwhile, some small species with D_h from 2.3 − 4.8 nm were observed, which might be attributed to the residual

of poly[2]pseudorotaxanes or even hexakis-pillar[5]arene metallacycles. Moreover, in order to further demonstrate the role of ditopic guest **G5** as the "cross-linking agent" in the formation of such supramolecular polymers, the Tyndall effect experiment was investigated as well. For example, the solution of **H2⊃(G5)$_3$** (pillar[5]arene unit = 7.5 × 10^{-5} M) in acetone exhibited a clear Tyndall effect, while in the case of **H1** (pillar[5]arene unit = 7.5 × 10^{-5} M) or **H2** (pillar[5]arene unit = 7.5 × 10^{-5} M) without the guest **G5** in acetone, no obvious Tyndall effect was observed (Figure S26 in SI). Similarly, a clear Tyndall effect was also found in the solution of **H3⊃(G5)$_3$** (pillar[5]arene unit = 7.5 × 10^{-5} M) rather than in the solution of **H1** or **H3** alone (Figure S27 in SI). These phenomena indicated that no obvious aggregates formed at this concentration for each host molecules **H1−H3** without the existence of neutral ditopic guest **G5**, thus providing the further proof for the role of **G5** as "cross-linking agent" during the formation of supramolecular polymers. Furthermore, the transmission electron microscopy (TEM) studies were performed, which provided the direct evidence for the existence of supramolecular polymerization of **H2⊃(G5)$_3$** and **H3⊃(G5)$_3$** and further insight into the morphological characteristics of cross-linked supramolecular polymers. As shown in Figure 8, the similar cross-linked three-dimensional
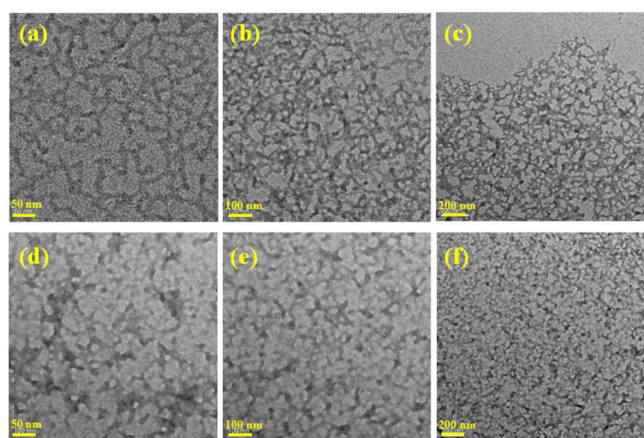
**Figure 8.** TEM images of cross-linked supramolecular polymers **H2⊃(G5)$_3$** (a−c) and **H3⊃(G5)$_3$** (d−f) in acetone.

(3-D) networks for both **H2⊃(G5)$_3$** and **H3⊃(G5)$_3$** systems were observed, respectively, which was consistent with the typical morphology of cross-linked supramolecular polymers.

Interestingly, the cross-linked supramolecular polymers can be destroyed by the addition of competitive guest adiponitrile due to the stronger binding ability between pillar[5]arene with adiponitrile than that of ditopic guest **G5**. ^{1}H NMR spectra (500 MHz, acetone-d_6, 295 K) were recorded to explore the disassembly of supramolecular polymers with the addition of competitive guest. As shown in Figure 9, all the main peaks of **H3⊃(G5)$_3$** became sharp gradually with the addition of competitive guest adiponitrile. It should be noted that the signals of free **G5** appeared after the addition of 1.0 eq competitive guest. For example, the phenyl protons H$_a$ and methylene protons H$_c$ in the free ditopic guest **G5** were found at 6.848 ppm and 2.473 ppm, respectively. Moreover, the signals of free **G5** got the maximum when the ratio of adiponitrile added up to 3.0 eq, representing that the original cross-linked supramolecular polymers were completely de-
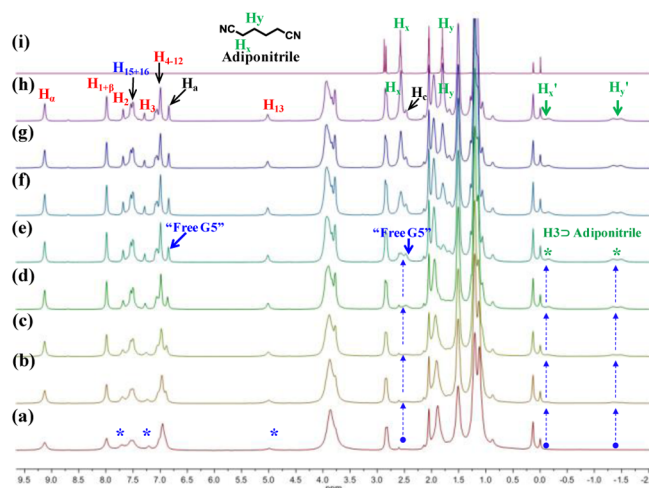
Figure 9. ^{1}H NMR spectra (500 MHz, acetone-d_6, 295 K) of **H3⊃(G5)$_3$** (20.0 mM) in the presence of adiponitrile: (a) 0 eq., (b) 0.25 eq., (c) 0.5 eq., (d) 1.0 eq., (e) 2.0 eq., (f) 3.0 eq., (g) 4.0 eq., and (h) 5.0 eq.; (i) adiponitrile.

stroyed and all the pillar[5]arene cavities were occupied by the competitive guest adiponitrile. At the same time, compared to the free axle, the signals for the methylene protons of the competitive guest exhibited upfield shifts and broadening effects (Δδ= −2.74 and −3.22 ppm for H$_x$ and H$_y$, respectively), which was illustrative of the formation of new poly[2]pseudorotaxanes based on the complexation between pillar[5]arene and adiponitrile. The same ^{1}H NMR experiment was carried out in the case of supramolecular polymer systems **H2⊃(G5)$_3$** (20 mM) and the similar observation was obtained as well (Figure S28 in SI). Furthermore, as indicated in Figure 10, with the addition of 5.0 eq of adiponitrile to the acetone-d_6
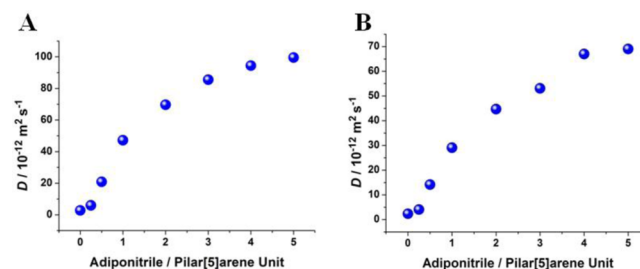
Figure 10. 2-D DOSY (500 MHz, 295 K) plot of acetone-d_6 solutions of **H2⊃(G5)$_3$** (20.0 mM) (A) and **H3⊃(G5)$_3$** (20.0 mM) (B) in the presence of 0, 0.25, 0.5, 1.0, 2.0, 3.0, 4.0, and 5.0 eq. competitive guest, respectively.

solutions of **H2⊃(G5)$_3$** (20 mM) or **H3⊃(G5)$_3$** (20 mM), the measured weight-average diffusion coefficients D of supramolecular aggregates increased dramatically from 2.80 × 10^{-12} to 9.95 × 10^{-11} m^2 s^{-1} and 2.36 × 10^{-12} to 6.90 × 10^{-11} m^2 s^{-1}, respectively, indicating the disassembly of cross-linked supramolecular polymer networks and the formation of new poly[2]pseudorotaxanes with small volume based on the complexation between pillar[5]arene and adiponitrile. The host−guest competition investigation gave clear evidence for the destruction of cross-linked supramolecular polymers by adding a competitive guest, which presented a successful example of the supramolecular transformation from cross-

linked supramolecular polymers to the discrete poly[2]-pseudorotaxanes.

Multiple Stimuli-Responsive Supramolecular Polymer Gels. It was found that both cross-linked supramolecular polymers $H2\supset(G5)_3$ and $H3\supset(G5)_3$ were able to transform into the stable supramolecular gels with different colors (bright yellow gels for $H2\supset(G5)_3$; orange gels for $H3\supset(G5)_3$) when the concentrations were increased to 23.1 mM and 22.3 mM, respectively (Figure 11). It should be noted that supra-
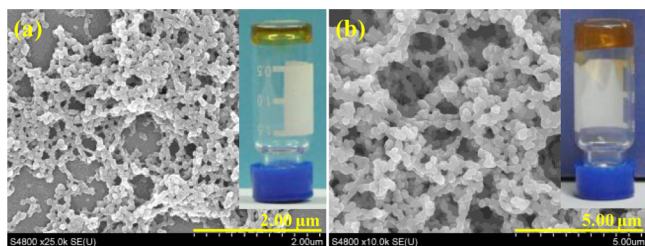
Figure 11. Photographs of gel formation in acetone and SEM images of the xerogel: (a) $H2\supset(G5)_3$ and (b) $H3\supset(G5)_3$.

molecular gels have played important roles in the development of soft material science.[27] Particularly, supramolecular polymer gels constructed through various driven force such as metal−ligand bonds, host−guest interactions, etc., have attracted considerable attention over recent years.[28] The critical gelator concentrations (CGCs) were determined to be 7.5 wt % for $H2\supset(G5)_3$ and 7.3 wt % for $H3\supset(G5)_3$ (in NMR tube, acetone, 295 K), respectively. The small difference of CGCs values between $H2\supset(G5)_3$ and $H3\supset(G5)_3$ indicated that the supramolecular polymer gels based on the large macrocycle host $H3$ featured somewhat stronger gelation ability than that of the small macrocycle host $H2$. The concentration-dependent ^1H NMR experiments were employed to probe the formation of supramolecular polymer gels, in which the obvious broadening effect of the main proton signals was observed, even some signals disappeared at 45.71 mM (Figure S29 in SI). This observation is consistent with the gradual enlargement of the supramolecular aggregates. Moreover, 2-D DOSY experiments were also carried out to investigate the formation of supramolecular polymer gels. For example, as the concentration of $H3\supset(G5)_3$ increased from 24.62 to 37.65 mM, the D value of supramolecular polymer gels decreased from 6.14×10^{-12} to 2.28×10^{-12} m^2 s^{-1} (Figure S30 in SI), indicating the formation of the larger polymer networks with the increase of concentration. It should be noted that all these NMR experiments were performed at 313 K in order to ensure that the gel was transformed into the solution, which could be detected by NMR. The morphologies of the xerogels were investigated by scanning electron microscopy (SEM). The similar three-dimensional (3-D) networks for both $H2\supset(G5)_3$ and $H3\supset(G5)_3$ xerogel systems were observed, which revealed the microstructures of cross-linked 3-D polymer networks (Figure 11 and Figures S31−S32 in SI). On the basis of all the above results, a possible explanation of such transformation from cross-linked supramolecular polymers to supramolecular gels was proposed. As shown in Scheme 3, with the continual increase of concentration, the cross-linked supramolecular polymers were first formed, which subsequently grew into the larger polymer networks and finally generated stable supramolecular polymer gels. It is not surprising that $H2\supset(G5)_3$ and $H3\supset(G5)_3$ have similar gel−sol properties except for the color

Scheme 3. Schematic Representation of the Formation of Supramolecular Polymer Gels
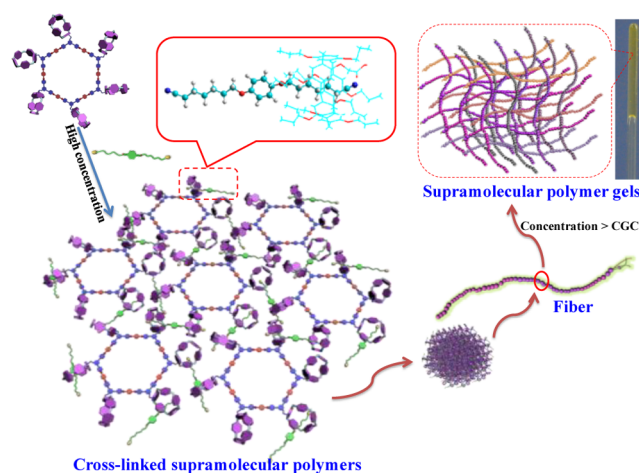


of gels and the gelation abilities, since metallacycle $H2$ and $H3$ owned very similar hexagonal scaffold and the polymer gels $H2\supset(G5)_3$ and $H3\supset(G5)_3$ featured the same gelation mechanism. To the best of our knowledge, this is one of the very few successful examples of supramolecular polymer gels constructed *via* the hierarchical self-assembly of pillar[n]arene derivatives.

Since this family of new cross-linked polymer gels was constructed from the 120° monofunctionalized pillar[5]arene derivatives *via* hierarchical self-assembly, inspired by the dynamic nature of metal−ligand bonds and host−guest interactions, the reversible multiple stimuli-responsive properties of such novel polymer gels were expected. Thus, the investigation of multiple stimuli-responsive behavior of the obtained supramolecular polymer gels was carried out.

It was found that these supramolecular gels were responsive to the temperature change. For instance, these stable gels of complexes $H2\supset(G5)_3$ or $H3\supset(G5)_3$ in acetone gradually became solutions when the temperature increased. Subsequently the gels were reformed as the solutions were cooled down to the room temperature (Figure 12). The determined gel-to-solution phase-transition temperature (T_{gel}) values of supramolecular polymers $H2\supset(G5)_3$ or $H3\supset(G5)_3$ in acetone was ~312 K. Further investigation revealed that the T_{gel} of both complexes $H2\supset(G5)_3$ and $H3\supset(G5)_3$ increased to be ~323 K when the concentration was over 60.00 mM (the concentration of pillar[5]arene unit), which revealed that the stability of the gel network was enhanced with the increase of the concentration.

Furthermore, because of the cross-linked supramolecular polymers could be destroyed in the presence of competitive dinitrile guests (demonstrated above), the reversible gel−sol transition through the adding and removing of competitive guest was anticipated. Upon adding 1.0 equiv adiponitrile (relative to the pillar[5]arene unit) into a gel sample of $H2\supset(G5)_3$ or $H3\supset(G5)_3$, it was found that the gel immediately collapsed and became a yellow solution (Figure 12). SEM investigation disclosed that the cross-linked networks morphology of supramolecular polymer gels was destroyed after the addition of adiponitrile, and an unordered blocky morphology was observed (Figure S35−S36 in SI). While upon adding a little excess of 1,4-bis(n-propoxy)pillar[5]arene[13d] (**DPP5**, as the competitive host) to the yellow solution, the
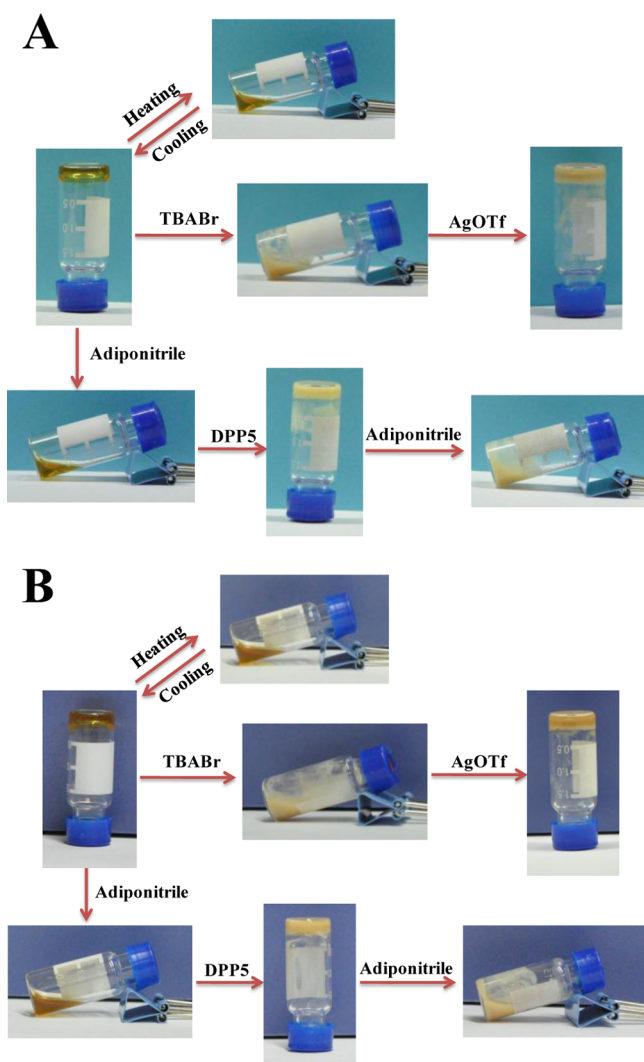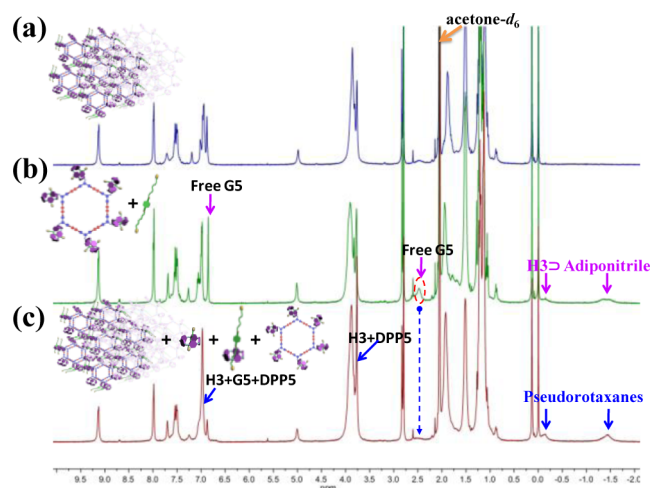
Figure 12. Reversible gel−sol transitions of supramolecular polymer gels triggered by a variety of stimuli for $H2 \supset (G5)_3$ (A) and $H3 \supset (G5)_3$ (B).

**Figure 13.** ^1H NMR spectra showing the disassembly and reassembly of polymer networks (400 MHz, 295 K, acetone-d_6): (a) supramolecular polymer $H3 \supset (G5)_3$, (b) after the addition of equimolar adiponitrile to $H3 \supset (G5)_3$, (c) after subsequent addition of equimolar **DPP5** to the mixture.

reformation of the supramolecular gel was realized. It should be noted that the reformed gels were pale yellow because the color of **DPP5** was white. SEM imaging also recorded the conversion from the unordered blocky morphology back to the cross-linked polymer networks (Figure S37−S38 in SI). As expected, the newly reformed pale-yellow gels can be transformed into solutions again upon subsequently adding the 1.0 equiv adiponitrile. SEM images also recorded such change of microstructures (Figure S39−S40 in SI).

In order to further demonstrate the stimuli-responsive gel−sol transition induced by the addition and removal of competitive guest, an *in situ* ^1H NMR investigation of $H2 \supset (G5)_3$ or $H3 \supset (G5)_3$ in acetone-d_6 was performed (Figure 13 and Figure S41 in SI). For example, upon adding adiponitrile to the solution of $H3 \supset (G5)_3$ in acetone-d_6, the signals of the free neutral ditopic guest **G5** were observed, and the signals of the newly generated poly[2]pseudorotaxanes based on the complexation between hexakis-pillar[5]arene metallacycles and adiponitrile were found, indicating the disassembly of supramolecular polymer networks. After the addition of **DPP5** to the mixture, the signals of free **G5** disappeared, and the original signals corresponding to the

cross-linked supramolecular polymers were restored, implying the reconstruction of cross-linked supramolecular polymers $H3 \supset (G5)_3$, which might mix with some other possible complexes, including $DPP5 \supset adiponitrile$, $DPP5 \supset G5$, and $H3 \supset adiponitrile$, etc. Such process of disassembly and reassembly of supramolecular polymers induced by adding and removing the competitive guests is presented in Scheme 4.

Recently, the applications of dynamic characteristics of coordination metal−ligand bonds[29] have been extensively explored in the area of multicomponent self-organization[30a,b] and supramolecular transformations.[7c,8f,22f,30c−e] Therefore, in this study, it is expected that the reversible stimuli-responsive gel−sol transition can be realized by taking advantages of the dynamic nature of Pt−N bonds, which can control the disassembly and reassembly of supramolecular metallacycle skeletons. It was found that the addition and removal of bromide ions (Br^{−}) led to the reversible gel−sol transitions in this study. As shown in Figure 12, upon adding 2 equiv of tetrabutylammonium bromide (**TBABr**) (relative to the pillar[5]arene unit) into the supramolecular polymer gels of $H2 \supset (G5)_3$ or $H3 \supset (G5)_3$, the gel gradually collapsed and ultimately became a turbid solution. It was proposed that the hexakis-pillar[5]arene metallacycles **H2** or **H3** was disassembled and the complex $H1 \supset G5$ was formed after the addition of **TBABr** (Scheme 4 and Figure S42 in SI). Because the complex $H1 \supset G5$ featured a poor solubility in acetone, a turbid solution rather than a clear, yellow solution was generated when the gel was destroyed. SEM images recorded that the large-scale, cross-linked networks of supramolecular polymer gels was destroyed after the addition of **TBABr** and an irregular morphology was observed (Figure S43−S44 in SI). However, after 4 equiv of silver trifluoromethanesulfonate (**AgOTf**) was added to the mixture, these turbid solutions were transformed into the stable polymer gels again (Figure 12 and Scheme 4). It was found that the AgBr precipitates were blackened during the process of supramolecular polymer gels regeneration since the AgBr is light sensitive, particularly under the heating conditions. SEM investigation also revealed the regeneration of the cross-linked polymer networks (Figure S45−S46 in SI).

Scheme 4. Schematic Representation of the Disassembly and Reassembly of Supramolecular Polymer Gels Induced by the Stimuli of Competitive Guest and Bromide Anion
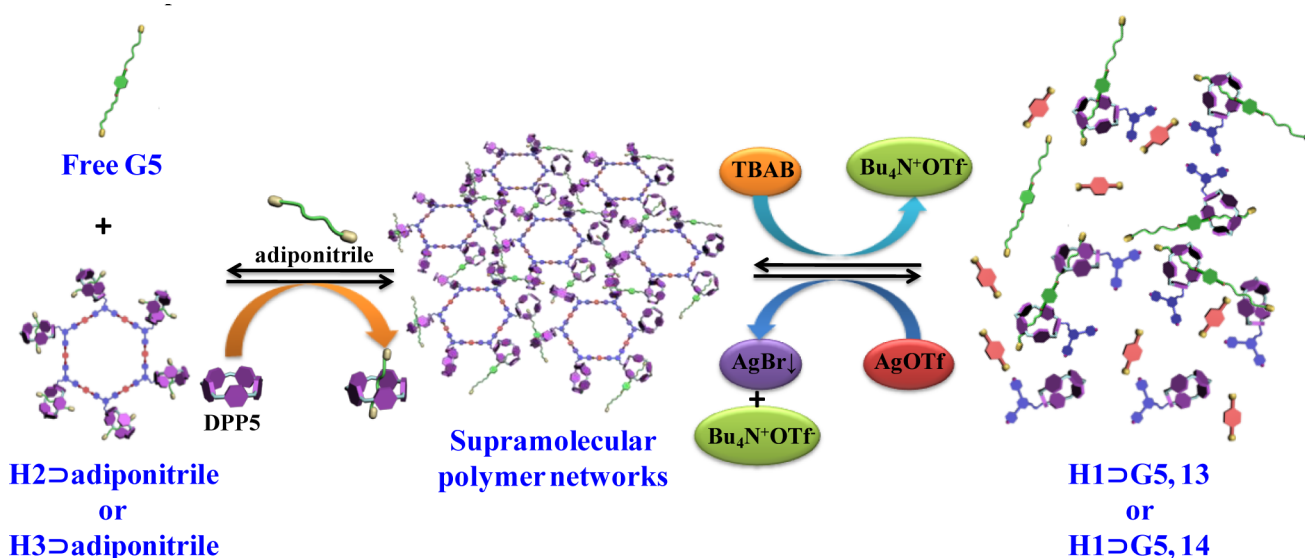
An *in situ* multinuclear NMR (^{1}H and ^{31}P) experiment of **H2⊃(G5)$_3$** or **H3⊃(G5)$_3$** in acetone-d_6 was carried out to further reveal the halide-induced reversible disassembly and reassembly of hexakis-pillar[5]arene metallacycles **H2–H3** (Scheme 4 and Scheme 5). As shown in Figure 14, after

Scheme 5. Stimuli-Responsive Disassembly and Reassembly of Hexakis-Pillar[5]arene Metallacycles H2 and H3 in Acetone Solution Induced by Bromide
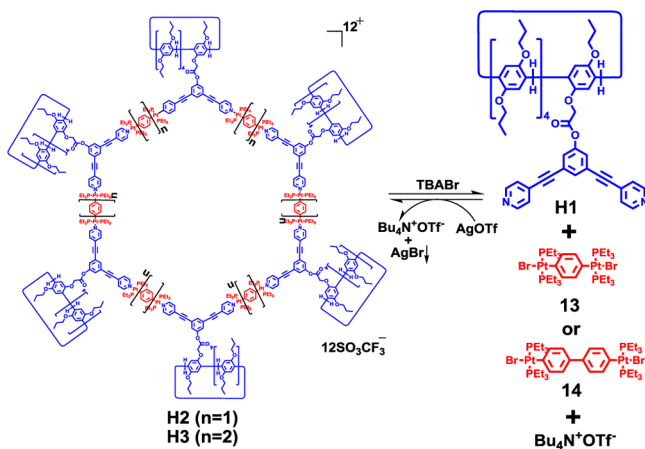
adding **TBABr** to the solution of **H3⊃(G5)$_3$**, the typical proton signals of hexakis-pillar[5]arene metallacycles **H3** disappeared. At the same time, the signals assigned to the complex **H1⊃G5** and a new Pt–Br complex **14** in a 1:1 ratio were found, which indicated the complete disassembly of hexakis-pillar[5]arene metallacycles **H3**. In addition, the formation of the new Pt–Br complex **14** was further confirmed by the increase of the coupling of flanking ^{195}Pt satellites ($\sim\Delta^1 J_{Pt-Pt} = 80.7$ Hz). As expected, the original hexakis-pillar[5]arene metallacycles **H3** were reassembled quantificationally after adding the AgOTf into the mixture (Figure 14). Similarly, an *in situ* multinuclear NMR experiment was employed to demonstrate the disassembly and reassembly process of supramolecular polymer networks **H2⊃(G5)$_3$** as well (Figure S47 in SI). All these

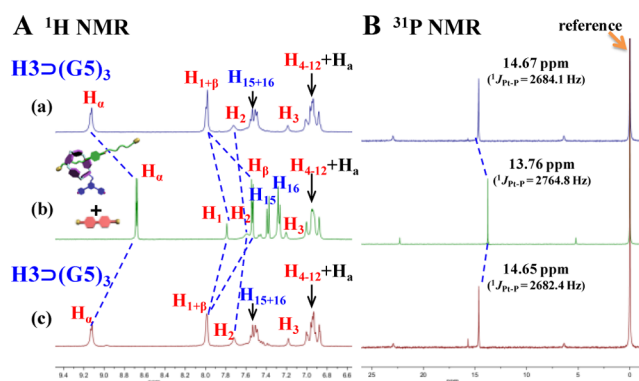**Figure 14.** (A) ^{1}H and (B) ^{31}P NMR spectra showing the disassembly and reassembly of supramolecular polymer networks (400 MHz, 295 K, acetone-d_6): (a) supramolecular polymer **H3⊃(G5)$_3$**, (b) after the addition of 2 equiv of **TBABr** to **H3⊃(G5)$_3$**, (c) after subsequent addition of 4 equiv of AgOTf to the mixture.

results supported that the halide-induced reversible disassembly and reassembly of hexagonal scaffold resulted in the reversible stimuli-responsive gel−sol transition in this study (Scheme 5).

3. CONCLUSIONS

In summary, we presented a highly efficient approach for the construction of multiple pillar[5]arene species. The novel 120° pillar[5]arene containing dipyridyl donor was designed and synthesized, from which a new family of hexakis-pillar[5]arene derivatives possessing a well-defined hexagonal metallacycle at their cores was successfully prepared through coordination-driven self-assembly. The synthesis is straightforward, and the yield is quantitative, thus eliminating the need of purification. All hexakis-pillar[5]arene metallacycles were well characterized with 1-D multinuclear NMR(^{1}H and ^{31}P), 2-D ^{1}H−^{1}H COSY and NOESY, ESI-TOF-MS, and elemental analysis. Their structural properties were studied by using PM6 semiempirical molecular orbital methods, which indicated that both hexakis-pillar[5]arene metallacycles featured very similar, roughly planar hexagonal rings with internal diameters of 5.0 and 5.8 nm, respectively. This research has once again proven the

versatility and modularity of coordination-driven self-assembly, which surely will be employed for the synthesis of other multiple pillar[n]arene analogues in the future.

The host−guest complexation of such hexakis-pillar[5]arene metallacycles with different neutral ditopic guests **G1−6** was investigated. Interestingly, the cross-linked supramolecular polymers were successfully constructed from multi-pillar[5]-arene metallacycles mainly driven by the intermolecular interactions between pillar[5]arene cavities and ditopic neutral dinitrile guests **G5** at the high concentration region. Furthermore, both cross-linked supramolecular polymers **H2⊃(G5)₃** and **H3⊃(G5)₃** could transform into the stable supramolecular gels when the concentrations were increased to a relatively high level. More importantly, by taking the advantages of the dynamic nature of metal−ligand bonds and host−guest interactions, reversible multiple stimuli-responsive gel−sol phase transition of such polymer gels was successfully realized. In addition, the reversible gel−sol transitions can be visualized macroscopically under the stimulations of temperature, halide, and competitive guest.

In a word, from the newly designed 120° pillar[5]arene containing dipyridyl precursor, a new class of multiple stimuli-responsive polymer gels were obtained *via* hierarchical self-assembly involving metal−ligand coordination and host−guest interactions. This study presents one of very few examples of multiple stimuli-responsive supramolecular polymer gels constructed from the discrete multiple pillar[n]arene derivatives, which not only enrich the library of higher-order supramolecular host−guest architectures and expand the application of hierarchical self-assembly but also provide a promising new method to prepare smart soft materials efficiently.

4. EXPERIMENTAL SECTION

Full experimental details are provided in the SI. The most important information is summarized briefly below.

General Information. Solvents were either employed as purchased or dried according to procedures described in the literature. ^{1}H NMR, ^{13}C NMR, ^{31}P NMR, and ^{19}F NMR spectra were recorded on Bruker 400 MHz Spectrometer ([1]H: 400 MHz; [13]C: 100 MHz; [31]P: 161.9 MHz) and Bruker 500 MHz Spectrometer ([1]H: 500 MHz) at 298 K. The ^{1}H and ^{13}C NMR chemical shifts are reported relative to residual solvent signals, and ^{31}P NMR resonances are referenced to an internal standard sample of 85% H_3PO_4 (δ 0.0). Coupling constants (J) are denoted in Hz and chemical shifts (δ) in ppm. Multiplicities are denoted as follows: s = singlet, d = doublet, m = multiplet, br = broad. Two-dimensional (2-D) [1]H−^{1}H COSY, NOESY, and DOSY were recorded on Bruker 500 MHz Spectrometer ([1]H: 500 MHz) at 295 K. IR spectra were recorded on a Bruker Tensor 27 infrared spectrophotometer.

Transmission Electron Microscopy (TEM) and Dynamic Light Scattering (DLS) Studies. TEM images were recorded on a Tecnai G² F30 (FEI Ltd.). The sample for TEM measurements was prepared by dropping the solution onto a carbon-coated copper grid. DLS measurements were performed under a Malvern Zetasizer Nano-ZS light scattering apparatus (Malvern Instruments, U.K.) with a He−Ne laser (633 nm, 4 mW).

Scanning Electron Microscopy (SEM) Experiments. The SEM samples were prepared on clean Si substrates. To minimize sample charging, a thin layer of Au was deposited onto the samples before SEM examination. All the SEM images were obtained using a S-4800 (Hitachi Ltd.) with an accelerating voltage of 3.0−10.0 kV.

Synthesis of Monofunctionalized Pillar[5]Arene 120° Pyridyl Donor H1. A 200 mL Schlenk flask charged with **1** (360 mg, 0.3437 mmol), **2** (112 mg, 0.3780 mmol), EDCI (79 mg, 0.4121 mmol), and HOBt (23 mg, 50 mol %), was degassed and backfilled three times

with N_2. Anhydrous dichloromethane (45 mL) was introduced into the reaction flask by syringe. The reaction was then stirred under an inert atmosphere at 0 °C for 2 min and 12 h at room temperature. The solvent was removed under reduced pressure. The residue was taken up in 30 mL CH_2Cl_2, washed twice with distilled water, and then dried over $MgSO_4$. After filtering, the solvent was removed by evaporation on a rotary evaporator. The residue was purified by column chromatography on silica gel (dichloromethane/ethyl acetate = 3/1) to give **H1** as a pale-yellow solid. Yield: 325 mg, 71.3%. R_f = 0.47 (dichloromethane/ethyl acetate = 2/1). Mp: 81−82 °C. ^{1}H NMR (CD_2Cl_2, 400 MHz): δ 8.62−8.63 (m, 4 H), 7.69−7.70 (m, 1 H), 7.41−7.42 (m, 6 H), 7.06 (s, 1 H), 6.97 (s, 1 H), 6.86−6.93 (m, 8 H), 4.84 (s, 2 H), 3.74−3.83 (m, 28 H), 1.78−1.95 (m, 18 H), 1.02−1.15 (m, 27 H); ^{13}C NMR (CD_2Cl_2, 100 MHz): δ 167.98, 151.15, 150.83, 150.50, 150.36, 150.31, 150.22, 150.18, 150.12, 150.06, 148.62, 133.32, 131.03, 129.21, 129.16, 129.00, 128.78, 128.67, 128.17, 126.07, 124.71, 115.11, 115.01, 114.74, 114.67, 114.64, 114.60, 114.53, 114.46, 91.72, 88.85, 70.53, 70.32, 66.21, 30.3, 30.18, 29.77, 29.68, 29.45, 29.34, 23.89, 23.75, 11.31, 11.21, 11.14, 11.09. IR (neat): 2967, 2956, 2937, 2868, 2840, 2363, 2216, 1792, 1763, 1598, 1498, 1474, 1406, 1390, 1276, 1261, 1205 cm^{-1}. LC/MS of **H1**: m/z calcd for $C_{84}H_{97}N_2O_{12}$ [M + H]$^+$: 1326.71, found: 1326.70; m/z calcd for $C_{84}H_{96}N_2NaO_{12}$ [M+Na]$^+$: 1348.69, found: 1348.15. MALDI-TOF-MS of **H1**: m/z calcd for $C_{84}H_{97}N_2O_{12}$ ([M+H]$^+$): 1326.71, found: 1326.69. Anal. Calcd for $C_{84}H_{96}N_2O_{12}$: C, 76.10; H, 7.30; N, 2.11. Found: C, 75.79; H, 7.289; N, 1.822.

Synthesis of the Small Multi-pillar[5]arene Hexagonal Metallocycle H2. The dipyridyl donor ligand **H1** (23.58 mg, 17.79 μmol) and the small organoplatinum 180° acceptor **3** (22.00 mg, 17.79 μmol) were weighed accurately into a glass vial. To the vial was added 2.6 mL DCM and 1.3 mL acetone. The reaction solution was then stirred at room temperature for 5 h to yield a homogeneous yellow solution. Yellow solid product **H2** was obtained by removing the solvent under vacuum. Yield: 45.58 mg, >99%. Mp: > 285 °C, dec. ^{1}H NMR (CD_2Cl_2, 400 MHz): δ 8.70 (d, 4 H, J = 5.2 Hz), 7.95 (s, 1 H), 7.82 (d, 4 H, J = 6.0 Hz), 7.55 (s, 2 H), 7.04−7.05 (m, 5 H), 6.98 (s, 1 H), 6.88−6.93 (m, 8 H), 4.88 (s, 2 H), 3.74−3.84 (m, 28 H), 1.81−1.95 (m, 18 H), 1.34−1.36 (m, 24 H), 1.06−1.17 (m, 63 H); ^{31}P NMR (CD_2Cl_2, 161.9 MHz): δ 13.17 (s, J_{Pt-P} = 2719.9 Hz); ^{19}F NMR (CD_2Cl_2, 376.5 MHz): δ −78.78 (s, 3F). ^{1}H NMR (acetone-d_6, 400 MHz): δ 9.06 (d, 4 H, J = 4.4 Hz), 7.96 (br, 5 H), 7.73 (s, 2 H), 7.15−7.20 (m, 5 H), 6.89−6.99 (m, 9 H), 4.96 (s, 2 H), 3.77−3.85 (m, 28 H), 1.84−1.86 (m, 18 H), 1.53 (br, 24 H), 1.05−1.21 (m, 63 H); ^{31}P NMR (acetone-d_6, 161.9 MHz): δ 14.11 (s, J_{Pt-P} = 2724.8 Hz); ^{19}F NMR (acetone-d_6, 376.5 MHz): δ 98.79 (s, 3F). IR (neat): 2962, 2941, 2926, 2370, 2345, 2326, 1788, 1450, 1410, 1269 cm^{-1}. ESI-TOF-MS of **H2**: calcd for [M − 11OTf]$^{11+}$: 1248.7343, found: 1248.7319; calcd for [M − 7OTf]$^{7+}$: 2047.4124, found: 2047.3915. Anal. Calcd for $C_{696}H_{960}F_{36}N_{12}O_{108}P_{24}Pt_{12}S_{12}$: C, 54.37; H, 6.29; N, 1.09. Found: C, 53.99; H, 6.43; N, 1.18.

Synthesis of the Big Multi-pillar[5]arene Hexagonal Metallocycle H3. The dipyridyl donor ligand **H1** (20.51 mg, 15.47 μmol) and the organoplatinum 120° acceptor **5** (20.32 mg, 15.47 μmol) were weighed accurately into a glass vial. To the vial was added 2.0 mL DCM and 2.0 mL acetone. The reaction solution was then stirred at room temperature for 5 h to yield a homogeneous yellow solution. Yellow solid product **H3** was obtained by removing the solvent under vacuum. Yield: 40.83 mg, >99%. Mp: > 280 °C, dec. ^{1}H NMR (CD_2Cl_2, 400 MHz): δ 8.71 (d, 4 H, J = 5.2 Hz), 7.97 (s, 1 H), 7.84 (d, 4 H, J = 5.2 Hz), 7.56 (s, 2 H), 7.41 (br, 8 H), 7.05 (s, 1 H), 6.98 (s, 1 H), 6.88−6.94 (m, 8 H), 4.89 (s, 2 H), 3.74−3.84 (m, 28 H), 1.81−1.96 (m, 18 H), 1.35−1.36 (m, 24 H), 1.05−1.18 (m, 63 H); ^{31}P NMR (CD_2Cl_2, 161.9 MHz): δ 13.92 (s, J_{Pt-P} = 2682.7 Hz); ^{19}F NMR (CD_2Cl_2, 376.5 MHz): δ −78.79 (s, 3F). ^{1}H NMR (acetone-d_6, 400 MHz): δ 9.13 (d, 4 H, J = 5.2 Hz), 7.98−7.80 (m, 5 H), 7.74 (s, 2 H), 7.49−7.56 (m, 8 H), 7.15 (s, 1 H), 6.89−6.99 (m, 9 H), 4.97 (s, 2 H), 3.76−3.90 (m, 28 H), 1.79−1.95 (m, 18 H), 1.51−1.52 (m, 24 H), 1.06−1.26 (m, 63 H); ^{31}P NMR (acetone-d_6, 161.9 MHz): δ 14.58 (s, J_{Pt-P} = 2682.7 Hz); ^{19}F NMR (acetone-d_6, 376.5 MHz): δ 98.77 (s, 3F). IR (neat): 3007, 2985, 2968, 1276, 1261, 1205, 1148 cm^{-1}. ESI-

TOF-MS of **H3**: calcd for $[M - 11OTf]^{11+}$: 1290.2112, found: 1290.2201; calcd for $[M - 7OTf]^{7+}$: 2112.7307, found: 2112.6904. Anal. Calcd for $C_{732}H_{984}F_{36}N_{12}O_{108}P_{24}Pt_{12}S_{12}$: C, 55.53; H, 6.26; N, 1.06. Found: C, 55.40; H, 6.32; N, 1.18.

■ ASSOCIATED CONTENT

ⓢ Supporting Information

Experimental details, NMR spectra, MS spectra, SEM images, and other supporting data. This material is available free of charge via the Internet at http://pubs.acs.org.

■ AUTHOR INFORMATION

Corresponding Author

hbyang@chem.ecnu.edu.cn

Notes

The authors declare no competing financial interest.

■ ACKNOWLEDGMENTS

■ REFERENCES

(1) (a) Kushner, D. J. *Bacteriol Rev.* **1969**, *33*, 302. (b) Neidle, S. *Oxford Handbook of Nucleic Acid Structure*; Oxford University Press: Oxford, 1999. (c) Jones, M. N.; Chapman, D. *Micelles, Monolayers, and Biomembranes*; Wiley-Liss: New York, 1995. (d) Kauffman, S. *At Home in the Universe: The Search for Laws of Self Organization and Complexity*; Oxford University Press: New York, 1995.

(2) (a) Choi, I. S.; Bowden, N.; Whitesides, G. M. *Angew. Chem., Int. Ed.* **1999**, *38*, 3078. (b) Elemans, J. A. A. W.; Rowan, A. E.; Nolte, R. J. M. *J. Mater. Chem.* **2003**, *13*, 2661. (c) Keizer, H. M.; Sijbesma, R. P. *Chem. Soc. Rev.* **2005**, *34*, 226.

(3) (a) Potschka, M.; Koch, M. H. J.; Adams, M. L.; Schuster, T. M. *Biochemistry* **1988**, *27*, 8481. (b) Prockop, D. J.; Fertala, A. *J. Struct. Biol.* **1998**, *122*, 111.

(4) (a) Hirschberg, J. H. K. K.; Brunsveld, L.; Ramzi, A.; Vekemans, J. A. J. M.; Sijbesma, R. P.; Meijer, E. W. *Nature* **2000**, *407*, 167. (b) Brunsveld, L.; Vekemans, J. A. J. M.; Hirschberg, J. H. K. K.; Sijbesma, R. P.; Meijer, E. W. *Proc. Natl. Acad. Sci. U.S.A.* **2002**, *99*, 4977. (c) Hartgerink, J. D.; Beniash, E.; Stupp, S. I. *Science* **2001**, *294*, 1684. (d) Fenniri, H.; Mathivanan, P.; Vidale, K. L.; Sherman, D. M.; Hallenga, K.; Wood, K. V.; Stowell, J. G. *J. Am. Chem. Soc.* **2001**, *123*, 3854. (e) Hill, J. P.; Jin, W.; Kosaka, A.; Fukushima, T.; Ichihara, H.; Shimomura, T.; Ito, K.; Hashizume, T.; Ishii, N.; Aida, T. *Science* **2004**, *304*, 1481. (f) Rzepecki, P.; Hochdörffer, K.; Schaller, T.; Zienau, J.; Harms, K.; Ochsenfeld, C.; Xie, X.; Schrader, T. *J. Am. Chem. Soc.* **2008**, *130*, 586. (g) Tancini, F.; Genovese, D.; Montalti, M.; Cristofolini, L.; Nasi, L.; Prodi, L.; Dalcanale, E. *J. Am. Chem. Soc.* **2010**, *132*, 4781. (h) Liu, J.; Chen, T.; Deng, X.; Wang, D.; Pei, J.; Wan, L.-J. *J. Am. Chem. Soc.* **2011**, *133*, 21010. (i) Cai, C.; Li, Y.; Lin, J.; Wang, L.; Lin, S.; Wang, X.-S.; Jiang, T. *Angew. Chem., Int. Ed.* **2013**, *52*, 7732. (j) Pfukwa, R.; Kouwer, P. H. J.; Rowan, A. E.; Klumperman, B. *Angew. Chem., Int. Ed.* **2013**, *52*, 11040.

(5) (a) Lehn, J.-M. *Supramolecular Chemistry: Concepts and Perspectives*; VCH: Weinheim, Germany, 1995. (b) Steed, J. W.; Atwood, J. L. *Supramolecular Chemistry*; John Wiley & Sons: West Sussex, U.K., 2000. (c) Steed, J. W.; Turner, D. R.; Wallace, K. J. *Core Concepts in Supramolecular Chemistry and Nanochemistry*; John Wiley & Sons: West Sussex, U.K., 2007. (d) Conn, M. M.; Rebek, J., Jr. *Chem. Rev.* **1997**, *97*, 1647. (e) Ajami, D.; Rebek, J., Jr. *Acc. Chem. Res.* **2013**, *46*, 990. (f) Raymo, F. M.; Stoddart, J. F. *Chem. Rev.* **1999**, *99*, 1643. (g) Forgan, R. S.; Sauvage, J.-P.; Stoddart, J. F. *Chem. Rev.* **2011**, *111*,

5434. (h) Brunsveld, L.; Folmer, B. J. B.; Meijer, E. W.; Sijbesma, R. P. *Chem. Rev.* **2001**, *101*, 4071.

(6) (a) Fujita, M.; Tominaga, M.; Hori, A.; Therrien, B. *Acc. Chem. Res.* **2005**, *38*, 369. (b) Pluth, M. D.; Raymond, K. N. *Chem. Soc. Rev.* **2007**, *36*, 161. (c) Liu, S.; Han, Y.-F.; Jin, G.-X. *Chem. Soc. Rev.* **2007**, *36*, 1543. (d) Oliveri, C. G.; Ulmann, P. A.; Wiester, M. J.; Mirkin, C. A. *Acc. Chem. Res.* **2008**, *41*, 1618. (e) Newkome, G. R.; Shreiner, C. *Chem. Rev.* **2010**, *110*, 6338. (f) Stang, P. J.; Olenyuk, B. *Acc. Chem. Res.* **1997**, *30*, 502. (g) Seidel, S. R.; Stang, P. J. *Acc. Chem. Res.* **2002**, *35*, 972. (h) Leininger, S.; Olenyuk, B.; Stang, P. J. *Chem. Rev.* **2000**, *100*, 853. (i) Chakrabarty, R.; Mukherjee, P. S.; Stang, P. J. *Chem. Rev.* **2011**, *111*, 6810. (j) Cook, T. R.; Zheng, Y.-R.; Stang, P. J. *Chem. Rev.* **2013**, *113*, 734. (k) Takezawa, Y.; Shionoya, M. *Acc. Chem. Res.* **2012**, *45*, 2066. (l) Yoshizawa, M.; Klosterman, J. K. *Chem. Soc. Rev.* **2014**, *43*, 1885.

(7) (a) Yoshizawa, M.; Tamura, M.; Fujita, M. *Science* **2006**, *312*, 251. (b) Yoshizawa, M.; Tamura, M.; Fujita, M. *Angew. Chem., Int. Ed.* **2007**, *46*, 3874. (c) Harano, K.; Hiraoka, S.; Shionoya, M. *J. Am. Chem. Soc.* **2007**, *129*, 5300. (d) Clever, G. H.; Tashiro, S.; Shionoya, M. *J. Am. Chem. Soc.* **2010**, *132*, 9973. (e) Freye, S.; Hey, J.; Torras-Galán, A.; Stalke, D.; Herbst-Irmer, R.; John, M.; Clever, G. H. *Angew. Chem., Int. Ed.* **2012**, *51*, 2191. (f) Freye, S.; Michel, R.; Stalke, D.; Pawliczek, M.; Frauendorf, H.; Clever, G. H. *J. Am. Chem. Soc.* **2013**, *135*, 8476. (g) Kishi, N.; Li, Z.; Yoza, K.; Akita, M.; Yoshizawa, M. *J. Am. Chem. Soc.* **2011**, *133*, 11438.

(8) (a) Fujita, M.; Yazaki, J.; Ogura, K. *J. Am. Chem. Soc.* **1990**, *112*, 5647. (b) Stang, P. J.; Cao, D. H. *J. Am. Chem. Soc.* **1994**, *116*, 4981. (c) Kryschenko, Y. K.; Seidel, S. R.; Arif, A. M.; Stang, P. J. *J. Am. Chem. Soc.* **2003**, *125*, 5193. (d) Yang, H.-B.; Das, N.; Huang, F.; Hawkridge, A. M.; Muddiman, D. C.; Stang, P. J. *J. Am. Chem. Soc.* **2006**, *128*, 10014. (e) Yang, H.-B.; Ghosh, K.; Zhao, Y.; Northrop, B. H.; Lyndon, M. M.; Muddiman, D. C.; White, H. S.; Stang, P. J. *J. Am. Chem. Soc.* **2008**, *130*, 839. (f) Zhao, L.; Northrop, B. H.; Stang, P. J. *J. Am. Chem. Soc.* **2008**, *130*, 11886. (g) Oliveri, C. G.; Gianneschi, N. C.; Nguyen, S. T.; Mirkin, C. A.; Stern, C. L.; Wawrzak, Z.; Pink, M. *J. Am. Chem. Soc.* **2006**, *128*, 16286. (h) Yoon, H. J.; Heo, J.; Mirkin, C. A. *J. Am. Chem. Soc.* **2007**, *129*, 14182. (i) Chen, T.; Pan, G.-B.; Wettach, H.; Fritzsche, M.; Höger, S.; Wan, L.-J.; Yang, H.-B.; Northrop, B. H.; Stang, P. J. *J. Am. Chem. Soc.* **2010**, *132*, 1328. (j) Kishi, N.; Akita, M.; Kamiya, M.; Hayashi, S.; Hsu, H.-F.; Yoshizawa, M. *J. Am. Chem. Soc.* **2013**, *135*, 12976.

(9) (a) Yan, X.; Li, S.; Pollock, J. B.; Cook, T. R.; Chen, J.; Zhang, Y.; Ji, X.; Yu, Y.; Huang, F.; Stang, P. J. *Proc. Natl. Acad. Sci. U.S.A.* **2013**, *110*, 15585. (b) Yan, X.; Li, S.; Cook, T. R.; Ji, X.; Yao, Y.; Pollock, J. B.; Shi, Y.; Yu, G.; Li, J.; Huang, F.; Stang, P. J. *J. Am. Chem. Soc.* **2013**, *135*, 14036. (c) Yan, X.; Jiang, B.; Cook, T. R.; Zhang, Y.; Li, J.; Yu, Y.; Huang, F.; Yang, H.-B.; Stang, P. J. *J. Am. Chem. Soc.* **2013**, *135*, 16813. (d) Zhao, G.-Z.; Chen, L.-J.; Wang, W.; Zhang, J.; Yang, G.; Wang, D.-X.; Yu, Y.; Yang, H.-B. *Chem.—Eur. J.* **2013**, *19*, 10094.

(10) (a) Pedersen, C. J. *Angew. Chem., Int. Ed. Engl.* **1988**, *27*, 1021. (b) Lehn, J.-M. *Angew. Chem., Int. Ed. Engl.* **1988**, *27*, 89. (c) Cram, D. J. *Angew. Chem., Int. Ed. Engl.* **1988**, *27*, 1009. (d) Szejtli, J. *Chem. Rev.* **1998**, *98*, 1743. (e) Dondoni, A.; Marra, A. *Chem. Rev.* **2010**, *110*, 4949. (f) Wang, M.-X. *Acc. Chem. Res.* **2012**, *45*, 182.

(11) (a) Ogoshi, T.; Kanai, S.; Fujinami, S.; Yamagishi, T. A.; Nakamoto, Y. *J. Am. Chem. Soc.* **2008**, *130*, 5022. (b) Ogoshi, T. *J. Inclusion Phenom. Macrocycl. Chem.* **2012**, *72*, 247. (c) Xue, M.; Yang, Y.; Chi, X.; Zhang, Z.; Huang, F. *Acc. Chem. Res.* **2012**, *45*, 1294. (d) Cragg, P. J.; Sharma, K. *Chem. Soc. Rev.* **2012**, *41*, 597. (e) Zhang, H.; Zhao, Y. *Chem.—Eur. J.* **2013**, *19*, 16862.

(12) (a) Ogoshi, T.; Umeda, K.; Yamagishi, T. A.; Nakamoto, Y. *Chem. Commun.* **2009**, 4874. (b) Ogoshi, T.; Shiga, R.; Hashizume, M.; Yamagishi, T. A. *Chem. Commun.* **2011**, *47*, 6927. (c) Zhang, Z.; Xia, B.; Han, C.; Yu, Y.; Huang, F. *Org. Lett.* **2010**, *12*, 3285. (d) Zhang, Z.; Luo, Y.; Chen, J.; Dong, S.; Yu, Y.; Ma, Z.; Huang, F. *Angew. Chem., Int. Ed.* **2011**, *50*, 1397. (e) Strutt, N. L.; Forgan, R. S.; Spruell, J. M.; Botros, Y. Y.; Stoddart, J. F. *J. Am. Chem. Soc.* **2011**, *133*, 5668. (f) Strutt, N. L.; Zhang, H.; Giesener, M. A.; Lei, J.; Stoddart, J. F. *Chem. Commun.* **2012**, *48*, 1647. (g) Duan, Q.; Xia, W.; Hu, X.; Ni,

M.; Jiang, J.; Lin, C.; Pan, Y.; Wang, L. *Chem. Commun.* **2012**, *48*, 8532.

(13) (a) Li, C.; Zhao, L.; Li, J.; Ding, X.; Chen, S.; Zhang, Q.; Yu, Y.; Jia, X. *Chem. Commun.* **2010**, *46*, 9016. (b) Ma, Y.; Chi, X.; Yan, X.; Liu, J.; Yao, Y.; Chen, W.; Huang, F.; Hou, J.-L. *Org. Lett.* **2012**, *14*, 1532. (c) Yu, G.; Han, C.; Zhang, Z.; Chen, J.; Yan, X.; Zheng, B.; Liu, S.; Huang, F. *J. Am. Chem. Soc.* **2012**, *134*, 8711. (d) Han, C.; Yu, G.; Zheng, B.; Huang, F. *Org. Lett.* **2012**, *14*, 1712. (e) Xia, W.; Hu, X.-Y.; Chen, Y.; Lin, C.; Wang, L. *Chem. Commun.* **2013**, *49*, 5085. (f) Li, C.; Han, K.; Li, J.; Zhang, H.; Ma, J.; Shu, X.; Chen, Z.; Weng, L.; Jia, X. *Org. Lett.* **2012**, *14*, 42. (g) Shu, X.; Chen, S.; Li, J.; Chen, Z.; Weng, L.; Jia, X.; Li, C. *Chem. Commun.* **2012**, *48*, 2967. (h) Shu, X.; Fan, J.; Li, J.; Wang, X.; Chen, W.; Jia, X.; Li, C. *Org. Biomol. Chem.* **2012**, *10*, 3393.

(14) (a) Ogoshi, T.; Nishida, Y.; Yamagishi, T. A.; Nakamoto, Y. *Macromolecules* **2010**, *43*, 7068. (b) Ogoshi, T.; Aoki, T.; Shiga, R.; Iizuka, R.; Ueda, S.; Demachi, K.; Yamafuji, D.; Kayama, H.; Yamagishi, T. A. *J. Am. Chem. Soc.* **2012**, *134*, 20322. (c) Zhang, Z.; Han, C.; Yu, G.; Huang, F. *Chem. Sci.* **2012**, *3*, 3026. (d) Dong, S.; Yuan, J.; Huang, F. *Chem. Sci.* **2014**, *5*, 247.

(15) (a) Yao, Y.; Xue, M.; Chen, J.; Zhang, M.; Huang, F. *J. Am. Chem. Soc.* **2012**, *134*, 15712. (b) Yu, G.; Ma, Y.; Han, C.; Yao, Y.; Tang, G.; Mao, Z.; Gao, C.; Huang, F. *J. Am. Chem. Soc.* **2013**, *135*, 10310−10313. (c) Li, H.; Chen, D.-X.; Sun, Y.-L.; Zheng, Y.; Tan, L.-L.; Weiss, P.; Yang, Y.-W. *J. Am. Chem. Soc.* **2013**, *135*, 1570. (d) Duan, Q.; Cao, Y.; Li, Y.; Hu, X.; Xiao, T.; Lin, C.; Pan, Y.; Wang, L. *J. Am. Chem. Soc.* **2013**, *135*, 10542.

(16) (a) Hu, X.-B.; Chen, Z.; Tang, G.; Hou, J.-L.; Li, Z.-T. *J. Am. Chem. Soc.* **2012**, *134*, 8384. (b) Si, W.; Chen, L.; Hu, X.-B.; Tang, G.; Chen, Z.; Hou, J.-L.; Li, Z.-T. *Angew. Chem., Int. Ed.* **2011**, *50*, 12564. (c) Chen, L.; Si, W.; Zhang, L.; Tang, G.; Li, Z.-T.; Hou, J.-L. *J. Am. Chem. Soc.* **2013**, *135*, 2152.

(17) (a) Yu, G.; Zhang, Z.; Han, C.; Xue, M.; Zhou, Q.; Huang, F. *Chem. Commun.* **2012**, *48*, 2958. (b) Sun, S.; Hu, X.-Y.; Chen, D.; Shi, J.; Dong, Y.; Lin, C.; Pan, Y.; Wang, L. *Polym. Chem.* **2013**, *4*, 2224.

(18) Strutt, N. L.; Fairen-Jimenez, D.; Iehl, J.; Lalonde, M. B.; Snurr, R. Q.; Farha, O. K.; Hupp, J. T.; Stoddart, J. F. *J. Am. Chem. Soc.* **2012**, *134*, 17436.

(19) (a) Guan, Y.; Ni, M.; Hu, X.; Xiao, T.; Xiong, S.; Lin, C.; Wang, L. *Chem. Commun.* **2012**, *48*, 8529. (b) Hu, X.-Y.; Wu, X.; Duan, Q.; Xiao, T.; Lin, C.; Wang, L. *Org. Lett.* **2012**, *14*, 4826. (c) Wang, X.; Han, K.; Li, J.; Jia, X.; Li, C. *Polym. Chem.* **2013**, *4*, 3998. (d) Li, C.; Han, K.; Li, J.; Zhang, Y.; Chen, W.; Yu, Y.; Jia, X. *Chem.—Eur. J.* **2013**, *19*, 11892. (e) Xia, B.; Zheng, B.; Han, C.; Dong, S.; Zhang, M.; Hu, B.; Yu, Y.; Huang, F. *Polym. Chem.* **2013**, *4*, 2019. (f) Ogoshi, T.; Kayama, H.; Yamafuji, D.; Aoki, T.; Yamagishi, T.-a. *Chem. Sci.* **2012**, *3*, 3221.

(20) (a) Ogoshi, T.; Demachi, T.; Kitajima, K.; Yamagishi, T.-a. *Chem. Commun.* **2011**, *47*, 10290. (b) Ogoshi, T.; Yoshikoshi, K.; Aoki, T.; Yamagishi, T.-a. *Chem. Commun.* **2013**, *49*, 8785. (c) Xia, B.; He, J.; Abliz, Z.; Yu, Y.; Huang, F. *Tetrahedron Lett.* **2011**, *52*, 4433. (d) Zhang, H.; Nguyen, K. T.; Ma, X.; Yan, H.; Guo, J.; Zhu, L.; Zhao, Y. *Org. Biomol. Chem.* **2013**, *11*, 2070.

(21) (a) Northrop, B. H.; Yang, H.-B.; Stang, P. J. *Chem. Commun.* **2008**, 5896. (b) Xu, L.; Chen, L.-J.; Yang, H.-B. *Chem. Commun.* **2014**, DOI: 10.1039/c3cc47484d.

(22) (a) Xu, X.-D.; Yang, H.-B.; Zheng, Y.-R.; Ghosh, K.; Lyndon, M. M.; Muddiman, D. C.; Stang, P. J. *J. Org. Chem.* **2010**, *75*, 7373. (b) Zhao, G.-Z.; Li, Q.-J.; Chen, L.-J.; Tan, H.; Wang, C.-H.; Lehman, D. A.; Muddiman, D. C.; Yang, H.-B. *Organometallics* **2011**, *30*, 3637. (c) Zhao, G.-Z.; Li, Q.-J.; Chen, L.-J.; Tan, H.; Wang, C.-H.; Wang, D.-X.; Yang, H.-B. *Organometallics* **2011**, *30*, 5141. (d) Chen, L.-J.; Li, Q.-J.; He, J.; Tan, H.; Abliz, Z.; Yang, H.-B. *J. Org. Chem.* **2012**, *77*, 1148. (e) Han, Q.; Wang, L.-L.; Li, Q.-J.; Zhao, G.-Z.; He, J.; Hu, B.; Tan, H.; Abliz, Z.; Yu, Y.; Yang, H.-B. *J. Org. Chem.* **2012**, *77*, 3426. (f) Chen, S.; Chen, L.-J.; Yang, H.-B.; Tian, H.; Zhu, W. *J. Am. Chem. Soc.* **2012**, *134*, 13596. (g) Wu, N.-W.; Zhang, J.; Ciren, D.; Han, Q.; Chen, L.-J.; Xu, L.; Yang, H.-B. *Organometallics* **2013**, *32*, 2536.

(23) (a) Liu, Y.; Wang, Z.; Zhang, X. *Chem. Soc. Rev.* **2012**, *41*, 5922. (b) Xu, H.; Cao, W.; Zhang, X. *Acc. Chem. Res.* **2013**, *46*, 1647. (c) Guo, D.-S.; Liu, Y. *Chem. Soc. Rev.* **2012**, *41*, 5907. (d) Appel, E. A.; Barrio, J. d.; Loh, X. J.; Scherman, O. A. *Chem. Soc. Rev.* **2012**, *41*, 6195. (e) Yan, X.; Wang, F.; Zheng, B.; Huang, F. *Chem. Soc. Rev.* **2012**, *41*, 6042.

(24) (a) Liu, Y.; Yu, Y.; Gao, J.; Wang, Z.; Zhang, X. *Angew. Chem., Int. Ed.* **2010**, *49*, 6576. (b) Liu, Y.; Huang, Z.; Tan, X.; Wang, Z.; Zhang, X. *Chem. Commun.* **2013**, *49*, 5766. (c) Sun, R.; Xue, C.; Ma, X.; Gao, M.; Tian, H.; Li, Q. *J. Am. Chem. Soc.* **2013**, *135*, 5990. (d) Appel, E. A.; Biedermann, F.; Rauwald, U.; Jones, S. T.; Zayed, J. M.; Scherman, O. A. *J. Am. Chem. Soc.* **2010**, *132*, 14251. (e) Dong, S.; Luo, Y.; Yan, X.; Zheng, B.; Ding, X.; Yu, Y.; Ma, Z.; Zhao, Q.; Huang, F. *Angew. Chem., Int. Ed.* **2011**, *50*, 1905. (f) Dong, S.; Zheng, B.; Xu, D.; Yan, X.; Zhang, M.; Huang, F. *Adv. Mater.* **2012**, *24*, 3191.

(25) (a) Stang, P. J.; Persky, N. E.; Manna, J. *J. Am. Chem. Soc.* **1997**, *119*, 4777. (b) Yang, H.-B.; Hawkridge, A. M.; Huang, S. D.; Das, N.; Bunge, S. D.; Muddiman, D. C.; Stang, P. J. *J. Am. Chem. Soc.* **2007**, *129*, 2120. (c) Ghosh, K.; Yang, H.-B.; Northrop, B. H.; Lyndon, M. M.; Zheng, Y.-R.; Muddiman, D. C.; Stang, P. J. *J. Am. Chem. Soc.* **2008**, *130*, 5320.

(26) Boinski, T.; Szumna, A. *Tetrahedron* **2012**, *68*, 9419.

(27) (a) Piepenbrock, M.-O. M.; Lloyd, G. O.; Clarke, N.; Steed, J. W. *Chem. Rev.* **2010**, *110*, 1960. (b) Tam, A. Y.-Y.; Yam, V. W.-W. *Chem. Soc. Rev.* **2013**, *42*, 1540.

(28) (a) Beck, J. B.; Rowan, S. J. *J. Am. Chem. Soc.* **2003**, *125*, 13922. (b) Weng, W.; Beck, J. B.; Jamieson, A. M.; Rowan, S. J. *J. Am. Chem. Soc.* **2006**, *128*, 11663. (c) Yan, X.; Xu, D.; Chi, X.; Chen, J.; Dong, S.; Ding, X.; Yu, Y.; Huang, F. *Adv. Mater.* **2012**, *24*, 362.

(29) Lehn, J.-M. *Chem. Soc. Rev.* **2007**, *36*, 151.

(30) (a) Northrop, B. H.; Zheng, Y.-R.; Chi, K.-W.; Stang, P. J. *Acc. Chem. Res.* **2009**, *42*, 1554. (b) Caulder, D. L.; Raymond, K. N. *Angew. Chem., Int. Ed.* **1997**, *36*, 1440. (c) Lusby, P. J.; Müller, P.; Pike, S. J.; Slawin, A. M. Z. *J. Am. Chem. Soc.* **2009**, *131*, 16398. (d) Brown, A. M.; Ovchinnikov, M. V.; Stern, C. L.; Mirkin, C. A. *J. Am. Chem. Soc.* **2004**, *126*, 14316. (e) Wang, P.; Moorefield, C. N.; Newkome, G. R. *Angew. Chem., Int. Ed.* **2005**, *44*, 1679.